nature ecology & evolution

Article

https://doi.org/10.1038/s41559-023-02265-9

Disease-driven top predator decline affects mesopredator population genomic structure

Received: 16 May 2023

Accepted: 2 November 2023

Published online: 08 January 2024

Check for updates

Marc A. Beer[1], Kirstin M. Proft[2], Anne Veillet[3], Christopher P. Kozakiewicz[4], David G. Hamilton[2], Rodrigo Hamede[2,5], Hamish McCallum[6], Paul A. Hohenlohe[7], Christopher P. Burridge[2], Mark J. Margres[8], Menna E. Jones[2] & Andrew Storfer[1]

Top predator declines are pervasive and often have dramatic effects on ecological communities via changes in food web dynamics, but their evolutionary consequences are virtually unknown. Tasmania's top terrestrial predator, the Tasmanian devil, is declining due to a lethal transmissible cancer. Spotted-tailed quolls benefit via mesopredator release, and they alter their behaviour and resource use concomitant with devil declines and increased disease duration. Here, using a landscape community genomics framework to identify environmental drivers of population genomic structure and signatures of selection, we show that these biotic factors are consistently among the top variables explaining genomic structure of the quoll. Landscape resistance negatively correlates with devil density, suggesting that devil declines will increase quoll genetic subdivision over time, despite no change in quoll densities detected by camera trap studies. Devil density also contributes to signatures of selection in the quoll genome, including genes associated with muscle development and locomotion. Our results provide some of the first evidence of the evolutionary impacts of competition between a top predator and a mesopredator species in the context of a trophic cascade. As top predator declines are increasing globally, our framework can serve as a model for future studies of evolutionary impacts of altered ecological interactions.

Large carnivores are declining globally, resulting in dramatic changes within their ecological communities[1,2]. Changes in top predator densities often lead to changes in densities and/or behaviours of species at lower trophic levels, thus revealing the occurrence of trophic cascades[3]. Of particular concern is release of mesopredators, which can lead to secondary declines at lower trophic levels[3–5]. Whereas density-mediated and trait-mediated ecological effects involved in trophic cascades have been well-documented, little is known about the evolutionary consequences of these altered ecological interactions[6]. The large home ranges and dispersal capabilities of top predators mean that

[1]School of Biological Sciences, Washington State University, Pullman, WA, USA. [2]School of Natural Sciences, University of Tasmania, Hobart, Tasmania, Australia. [3]Hilo Core Genomics Facility, University of Hawaii at Hilo, Hilo, HI, USA. [4]Department of Integrative Biology, Michigan State University, W.K. Kellogg Biological Station, Hickory Corners, MI, USA. [5]CANECEV, Centre de Recherches Ecologiques et Evolutives sur le Cancer, Montpellier, France. [6]Environmental Futures Research Institute, Griffith University, Nathan, Queensland, Australia. [7]Institute for Bioinformatics and Evolutionary Studies, University of Idaho, Moscow, ID, USA. [8]Department of Integrative Biology, University of South Florida, Tampa, FL, USA. e-mail: astorfer@wsu.edu

'eco-evolutionary trophic cascades'[7] and evolutionary feedbacks associated with other species interactions (for example, competition) should be studied at the landscape scale, but most studies at this scale focus on abiotic factors that impact gene flow and local adaptation[8,9]. To address this knowledge gap, an integrated approach that tests the combined effects of the abiotic and biotic environment on evolutionary processes—landscape community genomics[10]—is necessary.

Long-term data documenting the rapid decline of the Tasmanian devil (*Sarcophilus harrisii*; hereafter, the devil), Tasmania's top terrestrial predator, has provided a unique opportunity for eco-evolutionary study. Devil facial tumour disease (DFTD), a transmissible cancer, is nearly always fatal and has spread rapidly throughout Tasmania, causing dramatic devil declines[11]. The east-to-west spread of DFTD over 25 years has generated a gradient of reduction in devil densities superimposed on an abiotically heterogeneous landscape (Fig. 1a)[11]. Devil declines have revealed a trophic cascade involving density- and trait-mediated effects on several species, but the evolutionary effects remain unknown[12–16]. We focus on the spotted-tailed quoll (*Dasyurus maculatus*; hereafter, the quoll), a smaller (quolls: mean 1.7 kg females, 3.2 kg males[17,18]; devils: mean 6.4 kg females, 8.4 kg males[17,19]), competitively subordinate mesopredator that experiences mesopredator release characterized by shifts in ecological resource use and activity timing in association with devil declines (Fig. 1b)[14,20]. At pre-disease devil densities, devils and quolls exhibit partial dietary[14,20,21] and substantial temporal[15,22] niche partitioning indicative of interspecific competition, both of which become weaker following devil declines.

Devil populations typically remain at low densities following DFTD-mediated declines[11], such that the quoll has experienced altered resource availability and behaviour for up to 25 generations, probably providing sufficient lag time to detect evolutionary effects of mesopredator release[23]. We hypothesize that declines in devil density and the duration of DFTD presence (in quoll generations; hereafter, simply 'generations diseased') will alter quoll population genomic structure mediated by increased resource availability and reduced interspecific competition. Quoll population genomic structure may increase due to reduced dispersal resulting from increased habitat quality, and individual single nucleotide polymorphisms (SNPs) may experience selection due to altered competition intensity. We employed a landscape community genomics approach to test these hypotheses by quantifying how both biotic and abiotic environmental factors affect population genomic structure and signatures of selection in quolls. Using a dataset of 345 individual quolls genotyped at 3,431 SNPs, we implemented three general approaches to address these goals: (1) tests for a population genomic pattern of isolation-by-resistance (IBR)[24]; (2) tests for a population genomic pattern of isolation-by-environment (IBE)[25]; and (3) landscape genomic tests for selection at individual SNPs based on genetic–environment associations (GEAs)[26]. Tests for IBR characterize how environmental conditions across the landscape between locations affect population genomic structure by impeding or facilitating gene flow (for example, certain environmental conditions may act as obstacles to dispersal between locations)[24], whereas tests for IBE characterize how at-location environmental conditions influence population genomic structure as a consequence of selection against migrants from locations with different environmental conditions, or as a result of environmentally biased dispersal[25]. GEA tests identify significant associations between environmental conditions and allele frequencies at individual SNPs, thereby testing for genomic evidence of divergent selection (Fig. 1c).

Results

The environment between sites drives IBR

To understand the influence of the environment on quoll population genomic structure, it is first necessary to identify the number of genetic clusters represented in the dataset. fastSTRUCTURE[27] and discriminant analysis of principal components (DAPC)[28] showed strong agreement for $K = 3$ genetic clusters among our samples across Tasmania (Extended Data Fig. 1), with 98% of individuals sharing the same cluster of majority assignment in both methods (Fig. 2a and Extended Data Fig. 2a,b). The three genetic clusters were broadly oriented from east to west (Fig. 2a). Consistent with the broad results of the genetic clustering methods, an analysis of estimated effective migration surfaces (EEMS)[29] identified a geographic region characterized by low effective migration (that is, a statistic reflecting both local effective population size as well as gene flow) separating the eastern and western halves of Tasmania (Extended Data Fig. 3). Spatial variation in effective migration was also evident throughout Tasmania (Extended Data Fig. 3), which evidences a genomic pattern of IBR. IBR occurs when environmental conditions on the landscape between locations impede or facilitate dispersal and consequent gene flow[24].

Next, we used ResistanceGA[30] to further evaluate evidence for IBR and quantify the extent to which specific environmental factors contribute to IBR. Specifically, we tested for IBR driven by combinations of abiotic factors including climate, landcover classes, rivers and roads, as well as the biotic factor of devil density lagged by 5, 10, 15 and 20 quoll generations prior to quoll sample collection (Extended Data Table 2), thereby allowing a lag time to detect an evolutionary response. Resulting models indicated the greatest support (that is, lowest mean Akaike information criterion with small sample size correction (AICc) across 10,000 bootstraps with 70/30% training/test data split) for a model containing landcover classes and temperature diurnal range (statistical performance of a subset of 10 models with the lowest mean AICc are plotted in Fig. 2c–e; the total set of 100 models is plotted in Extended Data Fig. 4); this model had the best (that is, lowest) AICc in 90.93% of the bootstrap replicates and explained substantial variance in genetic distances among quolls (that is, marginal $R^2 = 64.36\%$). All other models had a mean ΔAICc > 2 relative to this model. A model containing temperature diurnal range and devil density lagged by 15 generations had worse mean AICc support but had the best AICc in 6.34% of bootstrap replicates; this model explained similar variance in genetic distances among quolls (marginal $R^2 = 66.61\%$) compared with the model with the lowest mean AICc. Notably, a model including devil density lagged by 10 quoll generations and mean annual temperature had the highest mean marginal R^2 (67.7%), although it did not have the lowest mean AICc. In models containing devil density, devil density was negatively correlated with landscape resistance for the quoll (Extended Data Fig. 4).

The local environment affects population genomic structure

We also tested for IBE using partial redundancy analysis (pRDA)[31] and generalized dissimilarity modelling (GDM) to determine whether at-location environmental conditions influence population genomic structure[32]. pRDA identified a significant effect of nine environmental factors on individual spatial genomic variation after accounting for geography and sampling date (adjusted $R^2 = 13.7\%$). These environmental factors included landcover classes, climate-related variables and generations diseased (Table 1). GDM revealed that geography and the environment together explained 55.9% of model deviance, with 14.5% attributable to the environment alone (Extended Data Fig. 5). Eight environmental factors had significant effects on individual pairwise genetic distances in GDM, including temperature seasonality ($P < 0.001$), precipitation seasonality ($P < 0.001$) and generations diseased ($P < 0.001$; Table 2 and Extended Data Fig. 6). Notably, 1.44% of model deviance was explained by generations diseased alone (Extended Data Fig. 5), although this variable is moderately confounded with temperature seasonality and temperature diurnal range (Extended Data Fig. 7).

Evidence for selection driven by abiotic and biotic factors

Given that the pattern of IBE may reflect natural selection[25], we also tested for signatures of divergent selection at individual SNPs using GEA analyses. GEA tests identified a total of 197 SNPs (5.7% of the total

https://doi.org/10.1038/s41559-023-02265-9

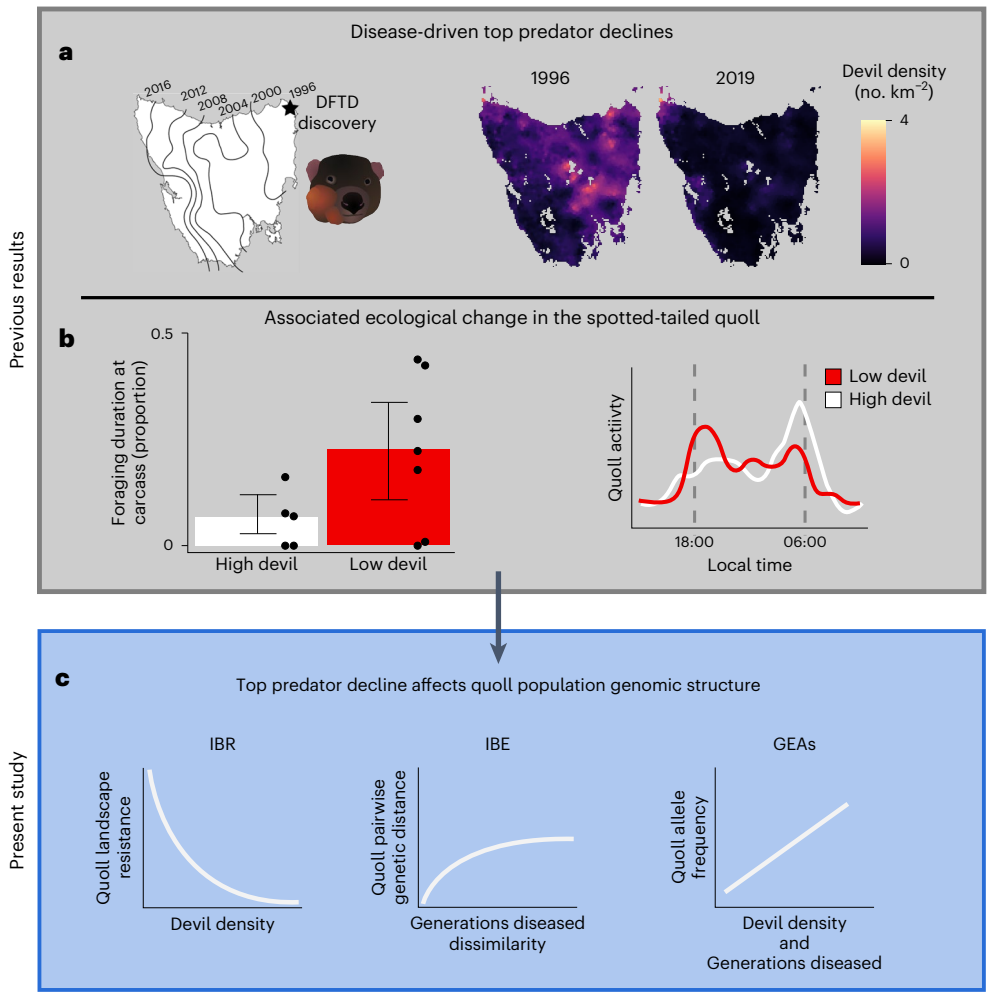

Fig. 1 | Research context of the present study. a, Left: DFTD was first discovered in the northeastern corner of Tasmania in 1996 (black star) and subsequently spread westwards across the island (black isolines indicate year of DFTD arrival). Right: DFTD has caused dramatic declines in local devil densities[4]. **b**, Devil declines result in ecological change to the spotted-tailed quoll, a mesopredator. Left: Quoll carcass use increases as devil density decreases. Proportion of foraging duration was determined for high-devil and low-devil conditions based on $n = 5$ field study sites and $n = 7$ field study sites, respectively; data are reported as mean values and error bars indicate 95% confidence intervals[16]. Right: quoll activity timing shifts by 12 hours[7]. **c**, Trends identified in the present study based on genomic data include identification of significant contributions of devil density to IBR (left), generations diseased to IBE (middle), and both devil density and generations diseased to signatures of selection (GEAs; right). IBR describes how environmental conditions between locations impact gene flow; here, devil density and landscape resistance are negatively correlated (that is, gene flow relatively high between locations separated by regions of higher devil density). IBE describes how environmental conditions at sites impact population genomic structure between them; here, locations that differ by how many quoll generations DFTD has been present (generations diseased) are more genetically divergent than locations with similar values of generations diseased. GEA tests identify individual loci with allele frequencies highly correlated with environmental conditions, providing evidence of selection; here, we identified SNPs with significant associations between allele frequencies and both devil density and generations diseased.

analysed) as having significant signatures of divergent selection. Specifically, implementation of pRDA as a GEA test[31] identified 92 SNPs with significant environmental associations while controlling for population genomic structure and temporal variation in sampling. A test using latent factor mixed models (LFMM)[33] identified 116 SNPs with significant environmental associations after accounting for population genomic structure, and 11 SNPs overlapped between the two methods. For both methods, the largest numbers of SNPs were detected in association with temperature seasonality, precipitation seasonality and annual precipitation (Extended Data Table 3). Most notably, devil density and generations diseased were associated with 12 and 10 SNPs, respectively, with no overlap.

Among the notable genes that mapped near SNPs associated with devil density, *C2CD2* has been associated with gait speed and physical performance in humans[34], and *KLF5* has been associated with skeletal muscle development and bodyweight regulation[35–37]. In relation to generations diseased, the candidate gene *CHL1* is associated with varying aspects of feeding behaviour[38–40] and neuroplasticity[41], *TTC7A* with feeding behaviour[42], and *KDM4A* with fertility and litter size[43]. A complete summary of candidate genes with significant abiotic and biotic environmental associations can be found in Supplementary Table 1.

Discussion

Using multiple complementary approaches, we show that declines in devil densities resulting from the spread of a lethal transmissible cancer have significant effects on evolutionary processes in the spotted-tailed quoll, a mesopredator and subordinate competitor. Previous work has shown that quolls benefit from mesopredator release via the decline of the competitively dominant devil[14,15]. Here, we included a time lag (in quoll generations) to test for an evolutionary response, and devil density and number of generations diseased were included in some top models explaining population genomic structure among quoll

https://doi.org/10.1038/s41559-023-02265-9

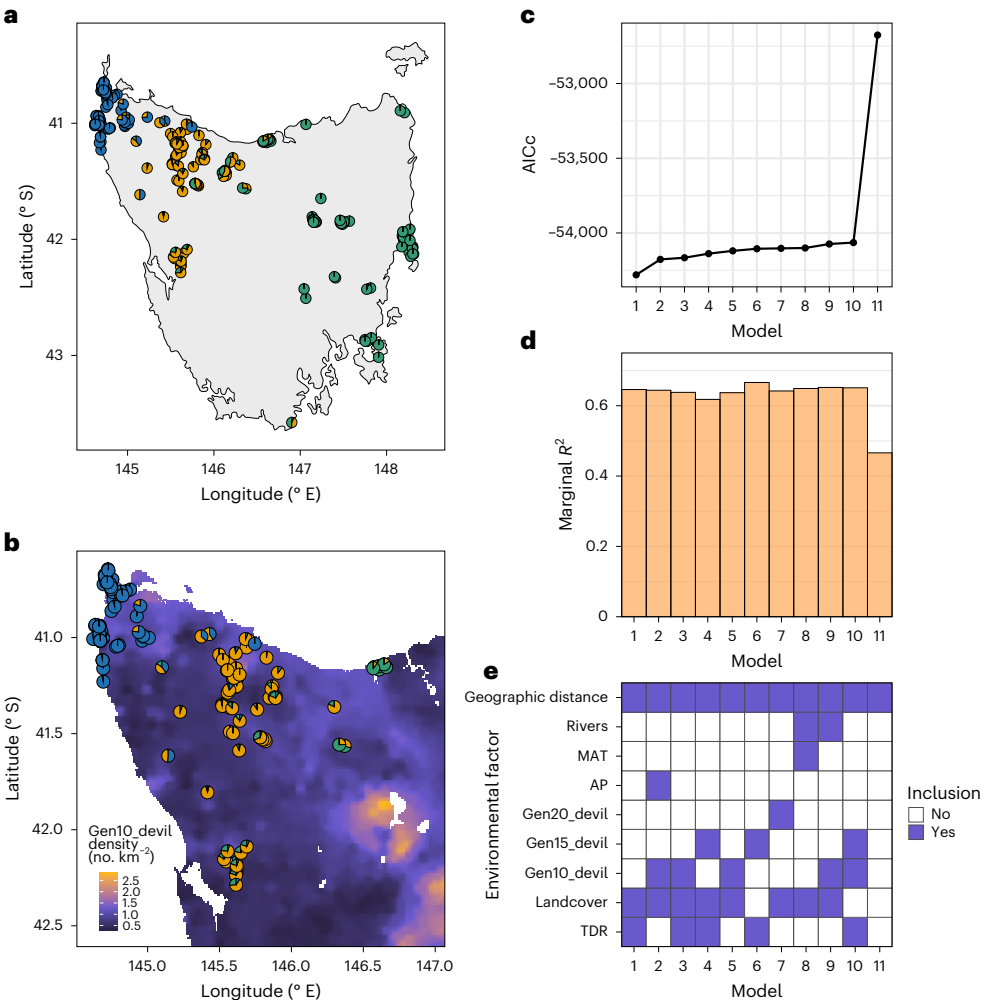

Fig. 2 | Population genomic structure of the spotted-tailed quoll across Tasmania. a, Map of fastSTRUCTURE ancestry proportions for all 345 individual quolls based on inference of three genetic clusters (that is, $K = 3$). Each individual is represented by a pie chart reflecting the proportion of ancestry assigned to each of the three genetic clusters. **b**, Individual fastSTRUCTURE ancestry proportions for the 189 individual quolls used in ResistanceGA plotted over devil density lagged by 10 generations. **c**–**e**, A subset of linear mixed-effects models with MLPE evaluating the contribution of abiotic and biotic variables to IBR, a spatial genomic pattern generated by environmental conditions between locations contributing to spatially variable resistance to gene flow across the landscape. Models are ordered left to right by increasing (worsening) average AICc based on 10,000 bootstrap replicates; that is, model 1 has the lowest AICc and is thus the best-performing model. **c**, Mean AICc of the ten models with the lowest AICc along with the null model of geographic distance. **d**, Marginal R^2 of the top-ranking models. Marginal R^2 is the proportion of variance in individual genetic distances explained by a resistance surface representing the composite of the indicated variables. **e**, Matrix indicating inclusion of environmental variables in models. Mean annual temperature (MAT), annual precipitation (AP), devil density lagged by 20, 15 and 10 quoll generations (Gen20_devil, Gen15_devil and Gen10_devil, respectively), landcover classes (TASVEG) and temperature diurnal range (TDR) are abbreviated in the matrix. Results for all 100 models are given in Extended Data Fig. 4.

localities. Devil density and generations diseased were also significantly correlated with allele frequencies at candidate loci putatively associated with predator avoidance and resource-use behaviour. Thus, disease-induced declines of Tasmania's top predator contribute to patterns of gene flow and selection in the quoll, thereby providing novel evidence of the evolutionary impacts of altered competitive interactions occurring within the broader context of a trophic cascade.

Although our tests for a population genomic pattern of IBR suggest a dominant effect of landcover classes, devil density may also contribute to IBR as it explains the greatest variation in genetic distances among quolls and appears in a top model based on AICc in a non-negligible fraction of bootstrap replicates[44]. The negative relationship between devil density and landscape resistance in IBR models indicates that quolls disperse less through areas of low devil density, possibly because such areas offer reduced competition and less dispersal pressure. That is, devil declines probably increase habitat quality for quolls because both species are nocturnal predators and scavengers with relatively high dietary overlap[20,21]. Low devil density increases the amount of carrion available to quolls[14] and simultaneously may reduce the chance of aggressive encounters between quolls and devils. Thus, dispersing quolls that encounter areas of low devil density and therefore low interspecific competition may not continue dispersing elsewhere, leading to low devil densities impeding gene flow and thereby increasing landscape resistance. Alternatively, telemetry data show that quoll and devil home ranges overlap at broad scales (88.4% overlap)[22], although core home ranges with higher usage intensity overlap less extensively (40.5% overlap)[22], probably because quolls prefer more forested or otherwise lower-visibility habitat than devils[21]. High devil densities probably occur where habitat is highly suitable for devils, and this habitat is probably highly suitable for quolls as well, given the broad overlap in the two species' space use. Highly suitable habitat may be relatively permissive to quoll dispersal

https://doi.org/10.1038/s41559-023-02265-9

Table 1 | pRDA variable importance for population genomic IBE

Variable	d.f.	Variance	*F*	*P*[a]
Elevation	1	0.387768	41.95973	0.001
Temperature diurnal range	1	0.332409	35.96949	0.001
Local per cent scrub habitat	1	0.288372	31.20430	0.001
Annual precipitation	1	0.233579	25.27520	0.001
Local per cent salt marsh/wetland	1	0.186797	20.21297	0.001
Generations diseased (DFTD)[b]	1	0.156495	16.93413	0.001
Local per cent dry eucalypt forest	1	0.135097	14.61864	0.001
Local per cent moorland habitat	1	0.102877	11.13215	0.003
Temperature seasonality	1	0.043770	4.736290	0.028
Residual	332	3.068151	NA[c]	NA[c]

[a]*P* values are based on an upper-tailed *F*-test. Significance testing was conducted on marginal terms at $\alpha = 0.05$ after model selection. We did not apply a multiple test correction. [b]Generations diseased refers to the number of quoll generations that DFTD has affected devils at a given time point and location. [c]The residual term is not subject to significance testing.

Table 2 | GDM variable importance for population genomic IBE

Variable	Importance[a]	*P*[b]
Temperature seasonality	10.11777	0
Precipitation seasonality	3.957330	0
Generations diseased (DFTD)	2.584018	0
Annual precipitation	1.432199	0.002
Geographic distance	1.027027	0
Local per cent eucalypt forest	1.016310	0.004
Local per cent rainforest	0.732745	0.010
Isothermality	0.608576	0.026
Local per cent human-modified habitat	0.315216	0.046

[a]Importance measures the per cent change in deviance explained by a model containing the observed data of all predictor variables and an equivalent model modified such that the predictor variable specified in a particular row of the table is represented by randomly permuted data. [b]The *P* value of a given predictor variable indicates the proportion of 500 models where randomly permuted predictor data outperformed the observed predictor data in terms of model deviance explained. That is, significance was determined using an upper-tailed permutation test of model deviance explained at $\alpha = 0.05$. We did not apply a multiple test correction.

and consequent gene flow, which may partly explain the negative correlation between quoll landscape resistance and devil density. Quolls may also avoid areas with high densities of feral cats, which increase in abundance concomitantly with declines of devils[16], although we have little evidence for quoll–cat interactions. Interestingly, the marginal R^2 achieved by the best-performing ResistanceGA model of IBR for quolls in our study (64.36%) is substantially higher than the marginal R^2 estimated in a study concerning IBR in Tasmanian devils (37.9%; driven largely by roads)[45]; this suggests that landscape resistance imposed by the environment may influence quoll gene flow more strongly than in its dominant competitor, although we note that the considerably greater spatial extent of our study may facilitate statistical detection of environmental drivers of genomic variation.

Our tests for a population genomic pattern of IBE indicate that quolls also disperse less among areas with differential local DFTD status, perhaps due to behavioural acclimation to a particular devil density. Although spatial avoidance between quolls and devils is weak[22], there is niche partitioning in the timing of peak activity levels when devils are present at relatively high densities[15,22]. When devils decline due to DFTD, quolls shift their timing of peak activity by approximately 12 hours to encroach on what was previously the devil's temporal niche[15], which represents a substantial behavioural shift that may discourage dispersal of quolls between geographic areas with divergent DFTD status. That is, quolls that have acclimated to geographic areas highly affected by DFTD (which have relatively low devil densities) may be less likely to disperse into areas less affected by DFTD (which typically have higher devil densities) and vice versa. Although the statistically significant effect estimated for generations diseased (which uniquely explains 1.44% of deviance in our final GDM model) is small, it is comparable to the variance explained by individual abiotic environmental factors in other vagile mammalian carnivores (for example, statistically significant abiotic environmental drivers of IBE in the American badger each uniquely explain <1% of genetic variance)[46]. Indeed, our final models for pRDA and GDM returned estimates for genetic variance explained collectively by environmental factors (pRDA: adjusted $R^2 = 13.7\%$; GDM: deviance explained 14.5%) that are similar to other mesopredator species, including bobcats (23.6% of genetic variance explained by variation in landcover)[47] and the American badger (8.15% of genetic variance explained collectively by topography and several abiotic environmental factors)[46].

We also found evidence suggesting that devil density and generations diseased generate divergent selection among sampling localities. GEA tests identified 12 SNPs significantly associated with devil density and 10 non-overlapping SNPs associated with generations diseased, suggesting these biotic variables impose distinct selection pressures. A structural equation model documenting trophic cascades supports this result via detection of significant effects of generations diseased independently from effects of current devil densities[14,16]. The candidate genes *C2CD2* and *KLF5*, found near SNPs associated with devil density in quolls, may reflect selection on physical performance associated with avoidance and escape of larger and behaviourally more dominant devils[48]. The candidate genes associated with generations diseased (that is, *CHL1*, *TTC7A* and *KDM4A*) are plausibly related to observed shifts in resource use and temporal activity of quolls driven by DFTD-induced devil declines[14,15,20]. The link between *KDM4A* and fertility[43] may reflect sustained changes to local abundances of quolls resulting from improved resource availability in diseased devil populations[14]. However, previous quoll abundance surveys did not show a change in quoll abundances[16], suggesting either (1) a transient population release that was later suppressed by competition with feral cats and avian species; or (2) a real population increase that was missed due to a lack of power to detect changes in quoll abundances via camera trap surveys. Notably, our results represent some of the first evidence for selection driven by indirect ecological interaction between a pathogen and a non-host taxon, a phenomenon that is expected to be widespread but difficult to study[6]. In addition to increasing evidence for selection resulting from direct interactions between species (for example, pathogen-imposed selection on hosts[49]; selection on predators associated with lethally toxic, novel pests[50]), we suggest that indirect ecological interactions may also broadly shape adaptive genomic variation in many species.

If devils and DFTD continue to coexist, models show that the local density of devils and prevalence of DFTD may cycle with a period of 5–20 years[51]. Given the association between devil densities, DFTD and evolutionary forces in quolls, devil–DFTD population cycling may lead to repeated perturbation of quoll population genomic structure in the future. The evolutionary consequences of reduced gene flow among quoll populations may be increased population fragmentation and reduced genetic diversity[52]. Alternatively, reduced gene flow may facilitate local adaptation[53] in cases where abiotic variables differ substantially among sites, such as precipitation at different altitudes across Tasmania.

Two caveats are worth noting. First, although multiple complementary analyses support the roles of spatiotemporal variation in devil density and generations diseased in explaining gene flow and selection

among quoll populations, these analyses are correlative and thus our results should not be interpreted as resolving causal relationships between variables. Second, although restriction-site associated DNA sequencing (RADseq) is powerful for characterizing environmental drivers of population genomic structure by inexpensively genotyping large numbers of individuals at several thousand genetic markers, the method yields a low density of genetic markers across the genome with which to test for selection[26,54]. As genome sequencing continues to decrease in cost, future studies may employ increased genome coverage to better characterize the genomic architecture underlying quoll local adaptation.

Despite the clear promise of landscape community genomics for pursuing an integrated understanding of the eco-evolutionary impacts of species interactions, few empirical studies exist in the literature. Notable insights from such an approach that would otherwise go undescribed include, for example, that spatiotemporal variation in the biotic factor of DFTD is more important than abiotic factors in shaping patterns of adaptive genomic variation in devils[49] and signatures of selection in northern quolls associated with lethally toxic cane toads spreading across the Australian mainland[50]. Although one other study, to our knowledge, showed that an obligate mutualism between the ant species *Atta texana* and the fungi it cultivates affects the population genomic structure of the ant[55], other studies found no evidence for relationships between the biotic environment and genomic variation[56,57]. The relative paucity of landscape community genomics studies can largely be attributed to logistical difficulties. While abiotic factors such as climatic variables are readily estimated using remote sensing, spatiotemporal variation in biotic factors such as species densities are considerably more difficult to characterize. Indeed, the analyses performed herein would have been impossible without 35 years of spatially continuous estimates of devil density and DFTD arrival times[11].

Genetic studies of the evolutionary impacts of the changing abiotic environment, including climate and land use change, have informed conservation efforts aimed at maintaining genetic diversity and gene flow across the landscape[8]. However, the impacts of changes to biotic communities on evolutionary processes are poorly understood. Owing to climate change, land use change and emerging infectious diseases, numerous other species are expected to have experienced biotically mediated changes in ecological interactions[1,2,58,59], with the evolutionary impacts of those changes remaining largely unstudied. We expect that our work will spearhead similar efforts in other systems and promote a greater bridging of ecology and evolution.

Methods

Sample collection and sequencing data processing

Ear biopsies were collected from 548 spotted-tailed quolls (*Dasyurus maculatus*; hereafter, the quoll) during ecological fieldwork. Quolls were caught in meat-baited traps made from polypropylene pipes also used for capturing Tasmanian devils (*Sarcophilus harrisii*; hereafter, the devil); details are described in ref. 60. All quolls caught were implanted with a subcutaneous microchip to allow individual identification and had a 3 mm biopsy (KAI MEDICAL) taken from the lower edge of their right ear. Samples span 15 generations (2004–2019; quolls have a generation time of approximately 1 year) and are geographically widespread. Broad geographic areas were generally repeatedly sampled over time, resulting in little geographic bias in the timing of sampling (linear model of collection year regressed against latitude and longitude; adjusted $R^2 = 0.021$, $F = 0.4697$, $P < 0.01$). Both quolls and devils are present in southwestern Tasmania, but rugged terrain makes the area largely inaccessible for fieldwork to collect samples; thus, southwestern Tasmania is not represented by samples in our dataset. Tissue sample collections were conducted in compliance with University of Tasmania Animal Ethics Permits (A0008588, A0010296, A0011696, A0013326, A0015835, A0018223, A0016789) and the Tasmania Department of Natural Resources and Environment Animal Ethics Committee.

We used the SbfI restriction enzyme in a single-digest RADseq protocol[61] to generate seven library pools of 96 samples each; 62 samples were duplicated as technical replicates among library pools. A total of 548 unique individuals were sequenced. We size-selected for 400–500 bp fragments. All seven library pools were sequenced together on a single NovaSeq S4 lane at the University of Oregon GC3 Facility using 150 bp paired-end sequencing. Sequencing generated a total of 6,122,805,452 raw reads. We trimmed the 2 bp from raw forward and reverse sequence reads using Cutadapt[62]. Next, we demultiplexed and cleaned the sequence data using the process_radtags module of Stacks v2.52[63], with the r, c, q and bestrad options specified. A total of 5,046,173,116 reads (82.42% of the total raw reads) were retained following demultiplexing and cleaning. We subsequently removed polymerase chain reaction duplicates using the Stacks clone_filter module.

We next aligned the processed sequence data to the Tasmanian devil reference genome mSarHar1.11[64] using bwa-mem[65] with default settings except a strengthened clipping penalty of 10. The devil and quoll belong to sister genera within the family Dasyuridae, suggesting that directly aligning sequence reads to the devil reference genome is a viable strategy for inferring RAD loci[66]. Supporting this expectation, processed sequence reads for each sample mapped robustly to the devil genome (mean proportion of reads aligning with MAPQ10 = 89.3%; s.d. = 2.5%); using the northern quoll (*Dasyurus hallucatus*) genome only marginally increased the per-sample number of reads with MAPQ10 (mean change + 0.60%; s.d. = 0.78%). Furthermore, the devil reference genome has substantially higher contiguity (contig N50 = 63.34 Mb; 445 contigs; 7 scaffolds) than the northern quoll genome (contig N50 = 91 kb; 479,471 contigs; 418,623 scaffolds), and thus the devil genome probably provides higher-quality positional information. After reference alignment, we removed unmapped reads and reads with MAPQ < 10 before inferring RAD loci using the gstacks module of Stacks.

We filtered the resulting dataset using the populations module of Stacks and VCFtools[67]. Specifically, we implemented an iterative filtering procedure that cycled and progressively strengthened several missing data filters[68]; this process can produce a final dataset with higher-quality SNPs and a larger number of retained individuals than applying each filter only once at a stringent threshold[69]. The full filtering procedure is detailed in Extended Data Table 1. Although studies often remove SNPs that have high missing data in the global dataset, we sought to prevent spatiotemporal bias in missing data. Accordingly, we removed SNPs that had high missing data in at least one of nine spatiotemporal groups of samples. These spatiotemporal sample groups were determined by first distributing samples into three spatial groups based on Universal Transverse Mercator (UTM) zone 55S eastings; samples were assigned to spatial groups by dividing the range of observed eastings into three bins of equal width (that is, samples between 299,982 and 403,135 m; samples between 403,135 and 506,288 m; and samples between 506,288 and 609,441 m). Next, samples within each of these three spatial groups were distributed into three temporal groups (leading to a total of nine spatiotemporal groups) by dividing the range of observed collection years into three bins of equal width (that is, samples from 2004 to 2009; 2009 to 2014; and 2014 to 2019). Samples lacking GPS coordinates were removed prior to iterative filtering. We did not remove individuals on the basis of relatedness, as there is little documented benefit of doing so, and consequences can include reduced statistical precision and power[70,71].

The final dataset consisted of 3,431 SNPs and 345 individuals, a sample size that exceeds recommendations for landscape genomics[72]. Individual sequencing depth averaged across SNPs was generally robust (mean = 40.80 reads per SNP; s.d. = 25.37; range = 8.22–162.98). SNP sequencing depth averaged across individuals was also generally high (mean = 41.95 reads per SNP per individual; s.d. = 16.83;

range = 19.38 – 551.87). Individual-level missing data were generally low (mean = 13.24%; s.d. = 13.29%; range = 2.36–49.99%) and positively skewed such that relatively few individuals had missing data rates near 50% (50th percentile = 6.56%; 90th percentile = 35.95%). SNP-level missing data were also generally low (mean = 13.24%; s.d. = 4.92%; range = 1.45–27.25%) but more symmetrically distributed around the mean (50th percentile = 13.04%; 90th percentile = 20.00%). In terms of the total genotype matrix (with dimensions equalling 345 individuals by 3,431 SNPs), 13.24% of genotypes were missing.

Detection of population genetic structure

We inferred the number of genetic clusters represented in the dataset using fastSTRUCTURE[27] and DAPC[28]. For fastSTRUCTURE, we tested $K = 1–20$ using 20 replicates each. We implemented DAPC using the R package adegenet[73]. We used the find.clusters function to determine the value of K, and we used the xVal method to determine the number of principal components to retain in the final analysis. Then, we selected the optimal value of K as that which maximized the marginal likelihood in fastSTRUCTURE and that which minimized the Bayesian information criterion in DAPC (Extended Data Fig. 1).

Environmental data processing

We carried out landscape genetics and genomics analyses to determine the extent to which heterogeneity in environmental factors relates to spatial patterns of population genomic structure. We collected data for ten abiotic variables: mean annual temperature, mean temperature diurnal range, isothermality, temperature seasonality, annual precipitation, precipitation seasonality, elevation, roads, rivers and landcover type. Elevation, as well as temperature- and precipitation-related variables, was obtained from WorldClim v2 at 30-arcsec resolution[74]. Roads were downloaded from Geoscience Australia (ga.gov.au) and categorized into principal, secondary and minor roads[45]. Roads are used for foraging and movement by the quoll[75]. We additionally downloaded watercourse data from Geoscience Australia and retained major and minor rivers. Landcover type was initially obtained from the TASVEG 4.0 dataset[76]; raster cells were reclassified from the 150 raw, highly specific landcover classes into 11 broad landcover classes (Extended Data Table 2). Landcover type appears important for explaining the distribution and relative abundance of the quoll, which is moderately arboreal and prefers forest versus other landcover types[13,21].

We additionally collected data for two biotic variables: devil density and the number of quoll generations DFTD has existed at a given location, a variable we refer to as 'generations diseased.' Devil density raster data for 1985–2019 were obtained directly from ref. 11, and the generations diseased variable was derived from the DFTD arrival year raster from ref. 11. Specifically, we calculated generations diseased as collection year of a given quoll sample minus year of DFTD arrival, with negative values converted to zeros. Although local devil density declines following DFTD arrival, devil density and generations diseased capture non-redundant information (Pearson's $|r| \leq 0.58$, depending on temporal lag of devil density used; Extended Data Fig. 7). Generations diseased may better capture community ecological changes associated with DFTD-driven devil declines (for example, shifts in local abundances of other species that have not been estimated island-wide)[13,16]. Indeed, devil density and duration of DFTD presence (here, 'generations diseased') have independent significant effects on the Tasmanian mammalian community[16]. See subsequent sections for details regarding further processing of environmental data for specific analyses, which is also summarized in Extended Data Table 2.

IBR

IBR has emerged in the landscape genetics literature as a framework for understanding the effects of environmental variation between sites (for example, barriers) on gene flow[24]. We used two approaches to evaluate IBR: EEMS[29] and a landscape genetics circuit-theory-based approach. EEMS uses departures from IBD under a stepping-stone model to identify geographic areas of high or low effective migration[29]. We repeated the analysis using 250-, 500- and 1,000-deme lattices to evaluate consistency in the observed effective migration patterns.

We evaluated the contributions of specific environmental variables (described above and in Extended Data Table 2) to population genomic structure using a circuit-theory-based approach implemented in the R package ResistanceGA[30]. Briefly, ResistanceGA uses a genetic algorithm to optimize resistance surfaces by varying parameters defining the transformation relating values of environmental variables and landscape resistance to gene flow. Parameter values that maximize the correlation between the resulting pairwise resistance distances and observed pairwise genetic distances are taken as optimal. ResistanceGA provides objective parameterizations of resistance surfaces rather than relying on potentially flawed expert opinion. We optimized resistance surfaces using random-walk commute times, which are equivalent to resistance distances estimated using the circuit-theory-based approach implemented in Circuitscape[77] while improving computational efficiency[30]. Briefly, circuit-theory-based approaches to IBR calculate resistance distances by integrating over all possible paths joining a pair of sites or individuals on the resistance surface. In contrast, least-cost path modelling identifies a single optimal path and therefore invokes the biologically unrealistic assumption that individuals have complete knowledge of the landscape[24]. ResistanceGA regresses observed pairwise genetic distances against pairwise random-walk commute times resulting from resistance surface optimization using linear mixed-effects models with maximum-likelihood population effects (MLPE); MLPE accounts for non-independence among pairwise observations[78]. Simulations indicate that linear mixed-effects models with MLPE and ResistanceGA specifically perform well in recovering true resistance surfaces governing gene flow[44,79]. To characterize pairwise individual genetic distances, we used the propShared function in adegenet to calculate the proportion of shared alleles between individuals and subsequently calculated the pairwise individual genetic distance D_{PS}[80]. D_{PS} was calculated without imputing missing data.

Landscape genetics analyses can be misled when there are large gaps in sampling[81], and we aimed to evaluate the extent to which different temporal lags of spatially continuous devil density estimates impact population genomic structure among locations (precluding simultaneous use of highly temporally disparate samples). Therefore, we subsampled our dataset to include 189 individuals from western-central Tasmania, which was more thoroughly sampled over the six-generation period of 2007–2012 (Fig. 2b). Landscape-level devil density estimates were averaged for years corresponding to 5-, 10-, 15- and 20-generation lags of the 189 samples; we incremented lags by five generations due to computational constraints associated with optimizing numerous models using ResistanceGA.

We optimized resistance surfaces representing different combinations of environmental variables. We first optimized 14 univariate models, a full model containing all 14 variables and a model containing geographic distance alone. As the optimization procedure used by ResistanceGA is computationally expensive, we next limited the number of variable combinations to be optimized by removing six variables contributing <1% to the resistance surface defined in the full model. For the remaining eight variables, we optimized multivariate models containing all combinations of two (28 models) and three variables (56 models). Note that models containing environmental variables implicitly account for geographic distance because the transformation of environmental variables to resistance values ensures a minimum resistance value of one[30]. In total, 100 models were optimized. To conduct model selection, we used the function Resist.boot to perform pseudo-bootstrapping of the 100 models. We used 10,000 bootstrap iterations, retaining 70% of the data for training in each iteration. The model with the lowest average AICc across bootstraps was taken as the top model; any models within ΔAICc < 2 of the top model were

considered as having similar statistical performance. We also used the percentage of bootstrap replicates for which a model had the lowest AICc to consider evidence for alternative models that do not necessarily have the lowest mean AICc[44].

IBE

IBE describes the circumstance in which environmental conditions at sites (that is, at sample locations) impact gene flow[25]. Environmental values associated with each sample coordinate were obtained as the mean value within a circular 6.26 km^2 geodesic buffer zone, which approximates the average quoll home range size[22]. Geodesic buffer zones were generated using the geobuffer_pts function in the R package geobuffer[82]. We converted the TASVEG categorical landcover data into 11 binary rasters using the r.reclass function in GRASS GIS[83] before calculating the proportion of each buffer zone occupied by a given landcover type. To avoid testing an excessive number of environmental variables while also acknowledging the expectation for time lags between environmental change and population genomic patterns[23,84], we retained only the devil densities found at each site 5, 10 and 15 generations prior to sample collection. Road and river data were not used when testing for IBE, as they are linear features expected to contribute to IBR but not IBE.

We implemented two methods for evaluating IBE: pRDA and GDM. pRDA is an ordination approach analogous to linear regression, which can be used to associate variables representing genetic variation with the environment while removing the effects of non-focal variables such as geography[31]. Prior to carrying out pRDA, we carried out spatial principal component analysis (sPCA) using the spca function in the R package adegenet[73]. We used a distance-based connection network with the maximum distance specified as 50% of the maximum observed distance between samples to account for the expectation that quolls are unlikely to disperse across the entire study area while still ensuring robust connectivity among nodes in the network. Missing data were imputed by the spca function using mean-value imputation. From the sPCA, we obtained spatially lagged scores of the first two global (positive) structures, which were subsequently used as the response variables in pRDA[46,47]. We implemented pRDA using the rda and ordiR2step functions in the R package vegan[85]. Specifically, we included the environmental factors as explanatory variables and included a conditioning matrix based on geographic coordinates and collection date as a decimal-formatted year; this conditioning matrix served to account for geography and the possibility of a signature of genetic drift or unobserved variable confounding the generations diseased variable across the 15 generations of sampling. We defined an initial model using all environmental factors and calculated variance inflation factors (VIFs) to evaluate multicollinearity; specifically, we calculated VIFs, removed the factor with the maximum VIF and recalculated VIFs until all retained variables had VIF < 10. Ultimately, all retained variables had VIF < 10 except for longitude (VIF = 11.46), and we opted to retain this variable because it represents geography and has its effects removed prior to estimating environmental effects. We used the ordiR2step function using 10,000 permutations to carry out forward variable selection; we defined the search scope based on a null model containing only the conditioning matrix and a full model containing the conditioning matrix plus all retained environmental factors. We performed significance testing of marginal terms using the function anova.cca and calculated adjusted R^2 using RsquareAdj.

We used the R package gdm[86] to carry out GDM. GDM fits regression models to test for associations between pairwise genetic distances (here, D_{PS}) and environmental distances, while accommodating nonlinear relationships using spline functions[32]. As described previously, we calculated D_{PS} without imputing missing data. We evaluated Pearson's correlation coefficients between each pair of environmental variables. For each pair of variables with $r > 0.80$, one variable was removed. We used 500 matrix permutations and backward elimination to evaluate significance of environmental factors. We identified the top model as the one including geographic distance and only the environmental factors with significant effects; this corresponded to a model containing the fewest terms with little change in deviance explained relative to the full model[45].

Tests for selection and candidate gene identification

We carried out two GEA analyses to identify SNPs with significant signatures of divergent selection: redundancy analysis (RDA)[31] and LFMM[33]. RDA has relatively high power and low false positive rate under a variety of demographic scenarios and selection strengths[31,87]. Although RDA can attain high power and low false positive rate when employed singly, inclusion of environmental factors that are not truly selective pressures in analysis can inflate the false positive rate; this can be remedied by overlapping detected SNPs with another GEA test, such as LFMM, at the expense of power[87]. Given that our study is exploratory (that is, there is little existing understanding of environmental factors contributing to spatially varying selection in the quoll), we employed both RDA and LFMM. Neither RDA nor LFMM permit missing data, so we imputed missing genotypes using the snmf function from the R package LEA[88]. Using $K = 3$, we ran 50 replicate runs and retained the run with the highest genotype prediction accuracy, as determined by minimum cross entropy, as the imputed genotype matrix.

With respect to RDA, we initially fitted a model containing all environmental factors processed for the IBE analyses and accounted for population genetic structure using a conditioning matrix containing individual PC1 and PC2 scores obtained using adegenet (that is, we employed pRDA). We also included collection year in this conditioning matrix because the estimation of the generations diseased variable is partially confounded with time of sample collection (see 'Environmental data processing'). After fitting the initial model, we removed covariates showing excessive collinearity by evaluating VIFs; we aimed to remove covariates one at a time until all remaining covariates had VIF < 10. Ultimately, all retained variables had VIF < 10 except for PC1 scores, which had a VIF of 14.86. We opted to retain PC1 despite its high VIF because it represents the main axis of population genomic structure, which is necessary to control for in GEA analyses. PC1 was specified in the conditioning matrix, so its effects are removed prior to estimation of environmental effects; this should tend to reduce the effect sizes of collinear environmental factors and thus lead to more conservative results regarding GEAs than if PC1 had been removed. We used a q value of 0.01 as our threshold for significance to detect outliers in RDA space. To identify the individual environmental factor that each outlier is most strongly associated with, we regressed individual genotypes at outlier SNPs against each environmental factor in binomial models, recording the environmental factor producing the highest McFadden's pseudo-R^2 (ref. 89). Note that previous implementations of this follow-up procedure have used simple linear models[87], which are not strictly appropriate for population or individual allele frequencies[90]. In the present study, binomial and simple linear models identified the same environmental factor for 77.2% of outlier SNPs; we presented results for the binomial models.

We implemented LFMM 2 using the R package lfmm[33]. LFMM uses several latent factors (equal to the K genetic clusters represented in the data; herein, $K = 3$ latent factors) to account for population genomic structure when testing for associations between alleles and environmental factors. We used the function lfmm_test to output a P value for each SNP; we used the function qvalue in the R package qvalue to estimate q values based on P values. SNPs with q values < 0.01 were identified as being significantly associated with environmental variation. We subsequently identified genes nearest each significant SNP using the bedtools closest command[91].

Reporting summary

Further information on research design is available in the Nature Portfolio Reporting Summary linked to this article.

Data availability

Raw sequence data and sample metadata necessary for reproducing the study have been deposited at NCBI under BioProject PRJNA922561 and BioSamples SAMN32664143–32664814. Any other relevant data can be found within the article and its Supplementary Information.

Code availability

Scripts for running analyses underlying this study's results are publicly available in a GitHub repository (https://github.com/marcabeer/stquoll_landscape_genomics).

References

1. Estes, J. A. et al. Trophic downgrading of planet Earth. *Science* **333**, 301–306 (2011).
2. Ripple, W. J. et al. Status and ecological effects of the world's largest carnivores. *Science* **343**, 1241484 (2014).
3. Ripple, W. J. et al. What is a trophic cascade? *Trends Ecol. Evol.* **31**, 842–849 (2016).
4. Ritchie, E. G. & Johnson, C. N. Predator interactions, mesopredator release and biodiversity conservation. *Ecol. Lett.* **12**, 982–998 (2009).
5. Jachowski, D. S. et al. Identifying mesopredator release in multi-predator systems: a review of evidence from North America. *Mammal. Rev.* **50**, 367–381 (2020).
6. Estes, J. A., Brashares, J. S. & Power, M. E. Predicting and detecting reciprocity between indirect ecological interactions and evolution. *Am. Nat.* **181**, S76–S99 (2013).
7. Wood, Z. T., Palkovacs, E. P. & Kinnison, M. T. Eco-evolutionary feedbacks from non-target species influence harvest yield and sustainability. *Sci. Rep.* **8**, 6389 (2018).
8. Manel, S. & Holderegger, R. Ten years of landscape genetics. *Trends Ecol. Evol.* **28**, 614–621 (2013).
9. Storfer, A., Patton, A. & Fraik, A. K. Navigating the interface between landscape genetics and landscape genomics. *Front. Genet.* **9**, 68 (2018).
10. Hand, B. K., Lowe, W. H., Kovach, R. P., Muhlfeld, C. C. & Luikart, G. Landscape community genomics: understanding eco-evolutionary processes in complex environments. *Trends Ecol. Evol.* **30**, 161–168 (2015).
11. Cunningham, C. X. et al. Quantifying 25 years of disease-caused declines in Tasmanian devil populations: host density drives spatial pathogen spread. *Ecol. Lett.* **24**, 958–969 (2021).
12. Hollings, T., Jones, M., Mooney, N. & Mccallum, H. Trophic cascades following the disease-induced decline of an apex predator, the Tasmanian devil. *Conserv. Biol.* **28**, 63–75 (2014).
13. Hollings, T., Jones, M., Mooney, N. & McCallum, H. Disease-induced decline of an apex predator drives invasive dominated states and threatens biodiversity. *Ecology* **97**, 394–405 (2016).
14. Cunningham, C. X. et al. Top carnivore decline has cascading effects on scavengers and carrion persistence. *Proc. R. Soc. B* **285**, 20181582 (2018).
15. Cunningham, C. X., Scoleri, V., Johnson, C. N., Barmuta, L. A. & Jones, M. E. Temporal partitioning of activity: rising and falling top-predator abundance triggers community-wide shifts in diel activity. *Ecography* **42**, 2157–2168 (2019).
16. Cunningham, C. X., Johnson, C. N. & Jones, M. E. A native apex predator limits an invasive mesopredator and protects native prey: Tasmanian devils protecting bandicoots from cats. *Ecol. Lett.* **23**, 711–721 (2020).
17. Jones, M. E. & Barmuta, L. A. Diet overlap and relative abundance of sympatric dasyurid carnivores: a hypothesis of competition. *J. Anim. Ecol.* **67**, 410–421 (1998).
18. Belcher, C. A. Demographics of tiger quoll (*Dasyurus maculatus maculatus*) populations in south-eastern Australia. *Aust. J. Zool.* **51**, 611–626 (2003).
19. Belkhir, S., Hamede, R., Thomas, F., Ujvari, B. & Dujon, A. M. Season, weight, and age, but not transmissible cancer, affect tick loads in the endangered Tasmanian devil. *Infect. Genet. Evol.* **98**, 105221 (2022).
20. Andersen, G. E., Johnson, C. N., Barmuta, L. A. & Jones, M. E. Dietary partitioning of Australia's two marsupial hypercarnivores, the Tasmanian devil and the spotted-tailed quoll, across their shared distributional range. *PLoS ONE* **12**, e0188529 (2017).
21. Jones, M. E. & Barmuta, L. A. Niche differentiation among sympatric australian dasyurid carnivores. *J. Mammal.* **81**, 434–447 (2000).
22. Andersen, G. E., Johnson, C. N. & Jones, M. E. Space use and temporal partitioning of sympatric Tasmanian devils and spotted-tailed quolls. *Austral Ecol.* **45**, 355–365 (2020).
23. Landguth, E. L. et al. Quantifying the lag time to detect barriers in landscape genetics. *Mol. Ecol.* **19**, 4179–4191 (2010).
24. McRae, B. H. Isolation by resistance. *Evolution* **60**, 1551–1561 (2006).
25. Wang, I. J. & Bradburd, G. S. Isolation by environment. *Mol. Ecol.* **23**, 5649–5662 (2014).
26. Rellstab, C., Gugerli, F., Eckert, A. J., Hancock, A. M. & Holderegger, R. A practical guide to environmental association analysis in landscape genomics. *Mol. Ecol.* **24**, 4348–4370 (2015).
27. Raj, A., Stephens, M. & Pritchard, J. K. fastSTRUCTURE: variational inference of population structure in large SNP data sets. *Genetics* **197**, 573–589 (2014).
28. Jombart, T., Devillard, S. & Balloux, F. Discriminant analysis of principal components: a new method for the analysis of genetically structured populations. *BMC Genet.* **11**, 94 (2010).
29. Petkova, D., Novembre, J. & Stephens, M. Visualizing spatial population structure with estimated effective migration surfaces. *Nat. Genet.* **48**, 94–100 (2016).
30. Peterman, W. E. ResistanceGA: an R package for the optimization of resistance surfaces using genetic algorithms. *Methods Ecol. Evol.* **9**, 1638–1647 (2018).
31. Capblancq, T. & Forester, B. R. Redundancy analysis: a Swiss army knife for landscape genomics. *Methods Ecol. Evol.* **12**, 2298–2309 (2021).
32. Fitzpatrick, M. C. & Keller, S. R. Ecological genomics meets community-level modelling of biodiversity: mapping the genomic landscape of current and future environmental adaptation. *Ecol. Lett.* **18**, 1–16 (2015).
33. Caye, K., Jumentier, B., Lepeule, J. & François, O. LFMM 2: fast and accurate inference of gene–environment associations in genome-wide studies. *Mol. Biol. Evol.* **36**, 852–860 (2019).
34. Heckerman, D. et al. Genetic variants associated with physical performance and anthropometry in old age: a genome-wide association study in the *ilSIRENTE* cohort. *Sci. Rep.* **7**, 15879 (2017).
35. Hayashi, S., Manabe, I., Suzuki, Y., Relaix, F. & Oishi, Y. Klf5 regulates muscle differentiation by directly targeting muscle-specific genes in cooperation with MyoD in mice. *eLife* **5**, e17462 (2016).
36. Pol, C. J. et al. Cardiac myocyte KLF5 regulates body weight via alteration of cardiac FGF21. *Biochim. Biophys. Acta* **1865**, 2125–2137 (2019).
37. Zhang, D.-H. et al. KLF5 regulates chicken skeletal muscle atrophy via the canonical Wnt/β-catenin signaling pathway. *Exp. Anim.* **69**, 430–440 (2020).
38. Krivoruchko, A., Yatsyk, O. & Kanibolockaya, A. New candidate genes of high productivity in North-Caucasian sheep using genome-wide association study (GWAS). *Anim. Gene* **23**, 200119 (2022).
39. Pasandideh, M., Rahimi-Mianji, G. & Gholizadeh, M. A genome scan for quantitative trait loci affecting average daily gain and Kleiber ratio in Baluchi Sheep. *J. Genet.* **97**, 493–503 (2018).

40. Xu, Z. et al. Combination analysis of genome-wide association and transcriptome sequencing of residual feed intake in quality chickens. *BMC Genomics* **17**, 594 (2016).
41. Fabbri, C. et al. Neuronal cell adhesion genes and antidepressant response in three independent samples. *Pharmacogenomics J.* **15**, 538–548 (2015).
42. Stegemiller, M. R., Ellison, M. J., Hall, J. B., Sprinkle, J. E. & Murdoch, B. M. Identifying genetic variants affecting cattle grazing behavior experiencing mild heat load. *Transl. Anim. Sci.* **5**, S61–S66 (2021).
43. Hernández-Montiel, W. et al. Genome-wide association study reveals candidate genes for litter size traits in Pelibuey sheep. *Animals* **10**, 434 (2020).
44. Winiarski, K. J., Peterman, W. E. & McGarigal, K. Evaluation of the R package 'ResistanceGA': a promising approach towards the accurate optimization of landscape resistance surfaces. *Mol. Ecol. Resour.* **20**, 1583–1596 (2020).
45. Kozakiewicz, C. P. et al. Comparative landscape genetics reveals differential effects of environment on host and pathogen genetic structure in Tasmanian devils (*Sarcophilus harrisii*) and their transmissible tumour. *Mol. Ecol.* **29**, 3217–3233 (2020).
46. Kierepka, E. M. & Latch, E. K. High gene flow in the American badger overrides habitat preferences and limits broadscale genetic structure. *Mol. Ecol.* **25**, 6055–6076 (2016).
47. Cancellare, I. A. et al. Multiscale patterns of isolation by ecology and fine-scale population structure in Texas bobcats. *PeerJ* **9**, e11498 (2021).
48. Jones, M. E. *Guild Structure of the Large Marsupial Carnivores in Tasmania*. PhD thesis, Univ. Tasmania (1995).
49. Fraik, A. K. et al. Disease swamps molecular signatures of genetic–environmental associations to abiotic factors in Tasmanian devil (*Sarcophilus harrisii*) populations. *Evolution* **74**, 1392–1408 (2020).
50. Von Takach, B. et al. Population genomics of a predatory mammal reveals patterns of decline and impacts of exposure to toxic toads. *Mol. Ecol.* **31**, 5468–5486 (2022).
51. Wells, K. et al. Individual and temporal variation in pathogen load predicts long-term impacts of an emerging infectious disease. *Ecology* **100**, e02613 (2019).
52. Frankham, R. Relationship of genetic variation to population size in wildlife. *Conserv. Biol.* **10**, 1500–1508 (1996).
53. Lenormand, T. Gene flow and the limits to natural selection. *Trends Ecol. Evol.* **17**, 183–189 (2002).
54. Lowry, D. B. et al. Breaking RAD: an evaluation of the utility of restriction site-associated DNA sequencing for genome scans of adaptation. *Mol. Ecol. Resour.* **17**, 142–152 (2017).
55. Smith, C. C. et al. Landscape genomics of an obligate mutualism: concordant and discordant population structures between the leafcutter ant *Atta texana* and its two main fungal symbiont types. *Mol. Ecol.* **28**, 2831–2845 (2019).
56. Parsley, M. B. et al. Multiple lines of genetic inquiry reveal effects of local and landscape factors on an amphibian metapopulation. *Landsc. Ecol.* **35**, 319–335 (2020).
57. Wenzel, M. A., Douglas, A., James, M. C., Redpath, S. M. & Piertney, S. B. The role of parasite-driven selection in shaping landscape genomic structure in red grouse (*Lagopus lagopus scotica*). *Mol. Ecol.* **25**, 324–341 (2016).
58. Daszak, P., Cunningham, A. A. & Hyatt, A. D. Emerging infectious diseases of wildlife—threats to biodiversity and human health. *Science* **287**, 443–449 (2000).
59. Buck, J. C. & Ripple, W. J. Infectious agents trigger trophic cascades. *Trends Ecol. Evol.* **32**, 681–694 (2017).
60. Hamede, R. K. et al. Transmissible cancer in Tasmanian devils: localized lineage replacement and host population response. *Proc. R. Soc. B* **282**, 20151468 (2015).
61. Ali, O. A. et al. RAD capture (Rapture): flexible and efficient sequence-based genotyping. *Genetics* **202**, 389–400 (2016).
62. Martin, M. Cutadapt removes adapter sequences from high-throughput sequencing reads. *EMBnet J.* **17**, 10–12 (2011).
63. Rochette, N. C., Rivera-Colón, A. G. & Catchen, J. M. Stacks 2: analytical methods for paired-end sequencing improve RADseq-based population genomics. *Mol. Ecol.* **28**, 4737–4754 (2019).
64. Stammnitz, M. R. et al. The evolution of two transmissible cancers in Tasmanian devils. *Science* **380**, 283–293 (2023).
65. Li, H. & Durbin, R. Fast and accurate long-read alignment with Burrows–Wheeler transform. *Bioinformatics* **26**, 589–595 (2010).
66. Westerman, M. et al. Phylogenetic relationships of dasyuromorphian marsupials revisited. *Zool. J. Linn. Soc.* **176**, 686–701 (2016).
67. Danecek, P. et al. The variant call format and VCFtools. *Bioinformatics* **27**, 2156–2158 (2011).
68. Beer, M. A., Kane, R. A., Micheletti, S. J., Kozakiewicz, C. P. & Storfer, A. Landscape genomics of the streamside salamander: implications for species management in the face of environmental change. *Evol. Appl.* **15**, 220–236 (2022).
69. O'Leary, S. J., Puritz, J. B., Willis, S. C., Hollenbeck, C. M. & Portnoy, D. S. These aren't the loci you're looking for: principles of effective SNP filtering for molecular ecologists. *Mol. Ecol.* **27**, 3193–3206 (2018).
70. Waples, R. S. & Anderson, E. C. Purging putative siblings from population genetic data sets: a cautionary view. *Mol. Ecol.* **26**, 1211–1224 (2017).
71. Peterman, W., Brocato, E. R., Semlitsch, R. D. & Eggert, L. S. Reducing bias in population and landscape genetic inferences: the effects of sampling related individuals and multiple life stages. *PeerJ* **4**, e1813 (2016).
72. Selmoni, O., Vajana, E., Guillaume, A., Rochat, E. & Joost, S. Sampling strategy optimization to increase statistical power in landscape genomics: a simulation-based approach. *Mol. Ecol. Resour.* **20**, 154–169 (2020).
73. Jombart, T. adegenet: a R package for the multivariate analysis of genetic markers. *Bioinformatics* **24**, 1403–1405 (2008).
74. Fick, S. E. & Hijmans, R. J. WorldClim 2: new 1-km spatial resolution climate surfaces for global land areas. *Int. J. Climatol.* **37**, 4302–4315 (2017).
75. Andersen, G. E., Johnson, C. N., Barmuta, L. A. & Jones, M. E. Use of anthropogenic linear features by two medium-sized carnivores in reserved and agricultural landscapes. *Sci. Rep.* **7**, 11624 (2017).
76. *TASVEG 4.0* (DPIPWE, 2020); https://nre.tas.gov.au/conservation/development-planning-conservation-assessment/planning-tools/monitoring-and-mapping-tasmanias-vegetation-(tasveg)/tasveg-the-digital-vegetation-map-of-tasmania
77. McRae, B. H., Dickson, B. G., Keitt, T. H. & Shah, V. B. Using circuit theory to model connectivity in ecology, evolution, and conservation. *Ecology* **89**, 2712–2724 (2008).
78. Clarke, R. T., Rothery, P. & Raybould, A. F. Confidence limits for regression relationships between distance matrices: estimating gene flow with distance. *J. Agric. Biol. Environ. Stat.* **7**, 361–372 (2002).
79. Shirk, A. J., Landguth, E. L. & Cushman, S. A. A comparison of regression methods for model selection in individual-based landscape genetic analysis. *Mol. Ecol. Resour.* **18**, 55–67 (2018).
80. Bowcock, A. M. et al. High resolution of human evolutionary trees with polymorphic microsatellites. *Nature* **368**, 455–457 (1994).
81. Oyler-McCance, S. J., Fedy, B. C. & Landguth, E. L. Sample design effects in landscape genetics. *Conserv. Genet.* **14**, 275–285 (2013).
82. Valentin, S. Geobuffer: R package for constructing geodesic buffers using metric radii. *GitHub* https://github.com/valentinitnelav/geobuffer (2019).

83. Neteler, M., Bowman, M. H., Landa, M. & Metz, M. GRASS GIS: a multi-purpose open source GIS. *Environ. Model. Softw.* **31**, 124–130 (2012).
84. Epps, C. W. & Keyghobadi, N. Landscape genetics in a changing world: disentangling historical and contemporary influences and inferring change. *Mol. Ecol.* **24**, 6021–6040 (2015).
85. Oksanen, J. et al. vegan: Community Ecology Package (2020); https://cran.r-project.org/web/packages/vegan/index.html
86. Fitzpatrick, M. C., Chhatre, V. E., Soolanayakanahally, R. Y. & Keller, S. R. Experimental support for genomic prediction of climate maladaptation using the machine learning approach Gradient Forests. *Mol. Ecol. Resour.* **21**, 2749–2765 (2021).
87. Forester, B. R., Lasky, J. R., Wagner, H. H. & Urban, D. L. Comparing methods for detecting multilocus adaptation with multivariate genotype–environment associations. *Mol. Ecol.* **27**, 2215–2233 (2018).
88. Frichot, E. & François, O. LEA: an R package for landscape and ecological association studies. *Methods Ecol. Evol.* **6**, 925–929 (2015).
89. McFadden, D. in *Frontiers in Econometrics* (ed. Zarembka, P.) 105–142 (Academic Press, 1974).
90. Warton, D. I. & Hui, F. K. C. The arcsine is asinine: the analysis of proportions in ecology. *Ecology* **92**, 3–10 (2011).
91. Quinlan, A. R. & Hall, I. M. BEDTools: a flexible suite of utilities for comparing genomic features. *Bioinformatics* **26**, 841–842 (2010).

Acknowledgements

We thank M. F. Lawrance, R. A. Kane, B. McCulloch, S. L. Bartel and R. M. Rautsaw for constructive comments during project development. Funding was provided by the National Science Foundation Division of Environmental Biology through grant NSF DEB 2027446 (A.S., M.J.M., H.M., M.E.J.), the National Institute of General Medical Sciences under the National Institutes of Health under the US Department of Health and Human Services through grant R01-GM126563-01 (A.S., P.A.H., H.M. and M.E.J.), and the National Science Foundation Graduate Research Fellowship Program under Award 1842493 (M.A.B.). Sample collection was additionally funded by the Australian Research Council through Discovery and Linkage Program grants LP130100949 (M.E.J.), DP110103069 (M.E.J., H.M.), DP110102656 (M.E.J., H.M.), LP0989613 (M.E.J.) and LP0561120 (M.E.J., H.M.), and a Future Fellowship (FT100100031) to M.E.J.

Author contributions

A.S., M.J.M., H.M. and M.E.J. devised the project. K.M.P., R.H., D.G.H. and C.P.B. contributed samples, and M.A.B., K.M.P. and C.P.K. carried out DNA extractions. A.V. completed RADseq DNA library preparations and, along with P.A.H., assisted genotyping. A.S. supervised the project and M.A.B. carried out all analyses. M.A.B. and A.S. drafted the paper, and all authors contributed to the final version.

Competing interests

The authors declare no competing interests.

Additional information

Extended data is available for this paper at https://doi.org/10.1038/s41559-023-02265-9.

Supplementary information The online version contains supplementary material available at https://doi.org/10.1038/s41559-023-02265-9.

Correspondence and requests for materials should be addressed to Andrew Storfer.

Peer review information *Nature Ecology & Evolution* thanks the anonymous reviewers for their contribution to the peer review of this work. Peer reviewer reports are available.

https://doi.org/10.1038/s41559-023-02265-9

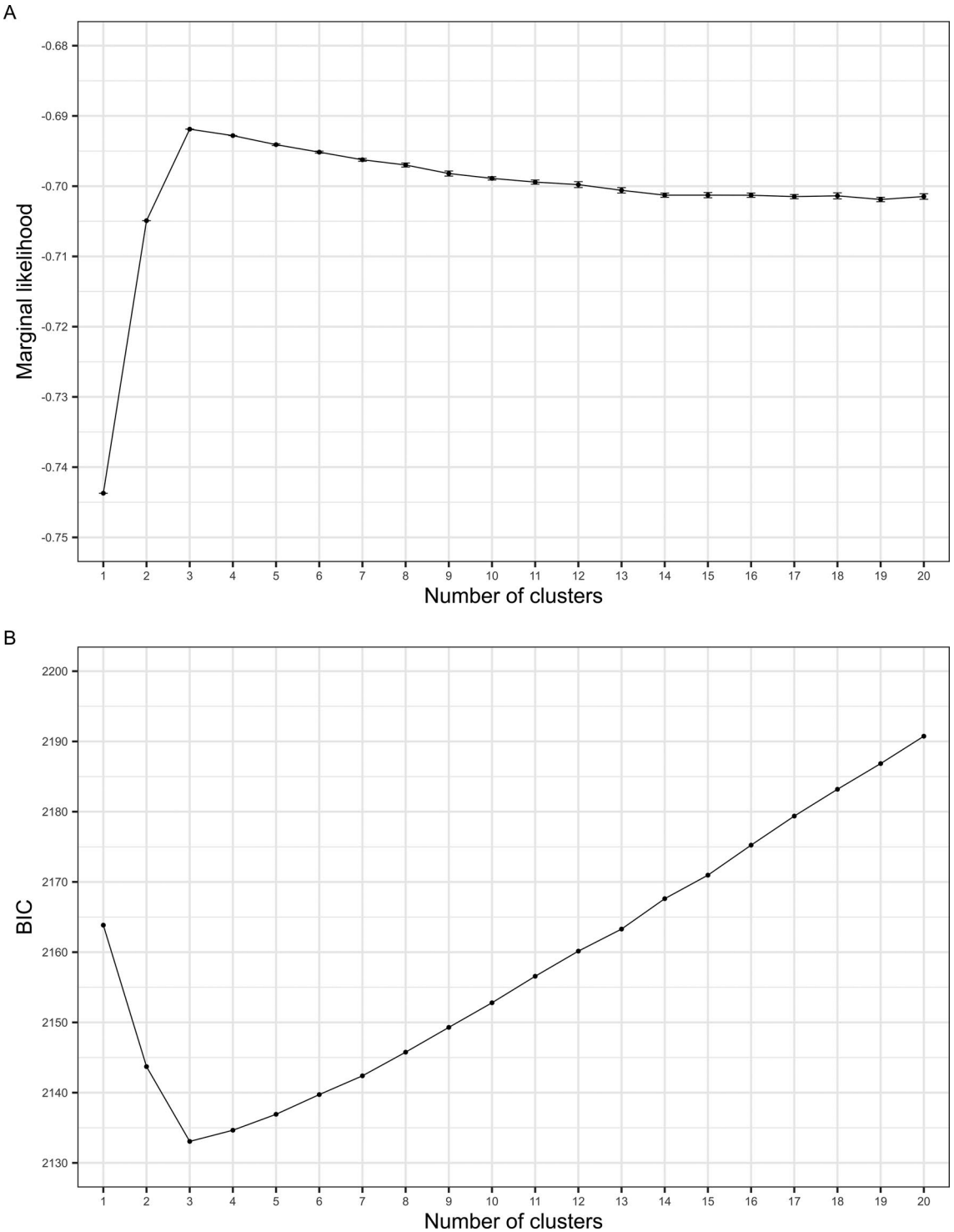

Extended Data Fig. 1 | Relative support for different values of K. Optimal K was determined by **a**) maximum marginal likelihood in FastStructure and **b**) minimum BIC in DAPC. Error bars in A indicate standard error across replicates.

https://doi.org/10.1038/s41559-023-02265-9

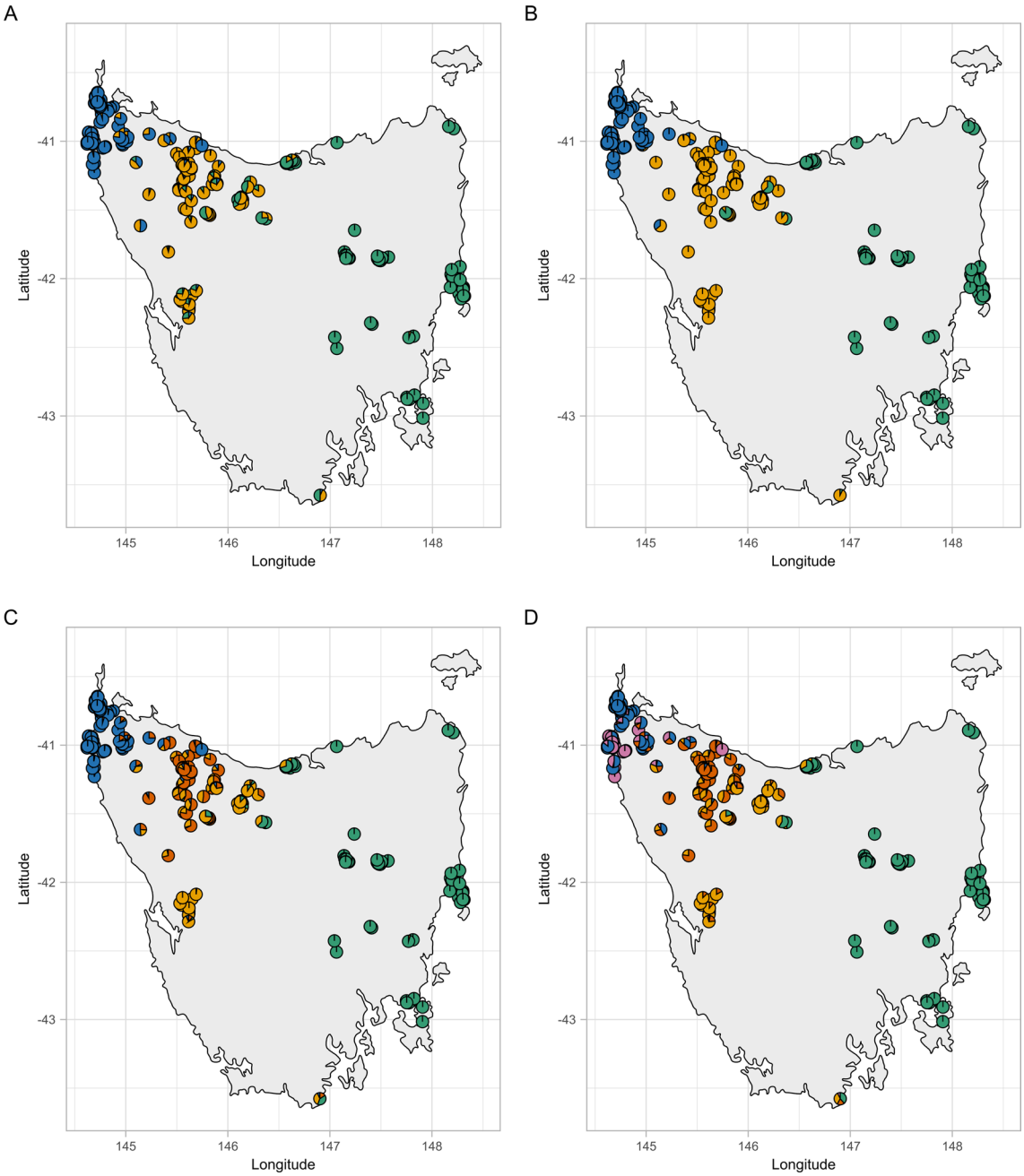

Extended Data Fig. 2 | Population genomic structure across Tasmania. a) FastStructure results for K = 3. **b**) DAPC results for K = 3. **c, d**) FastStructure results for K = 4-5. Each individual is represented by a pie chart reflecting the proportion of ancestry assigned to each genetic cluster.

https://doi.org/10.1038/s41559-023-02265-9

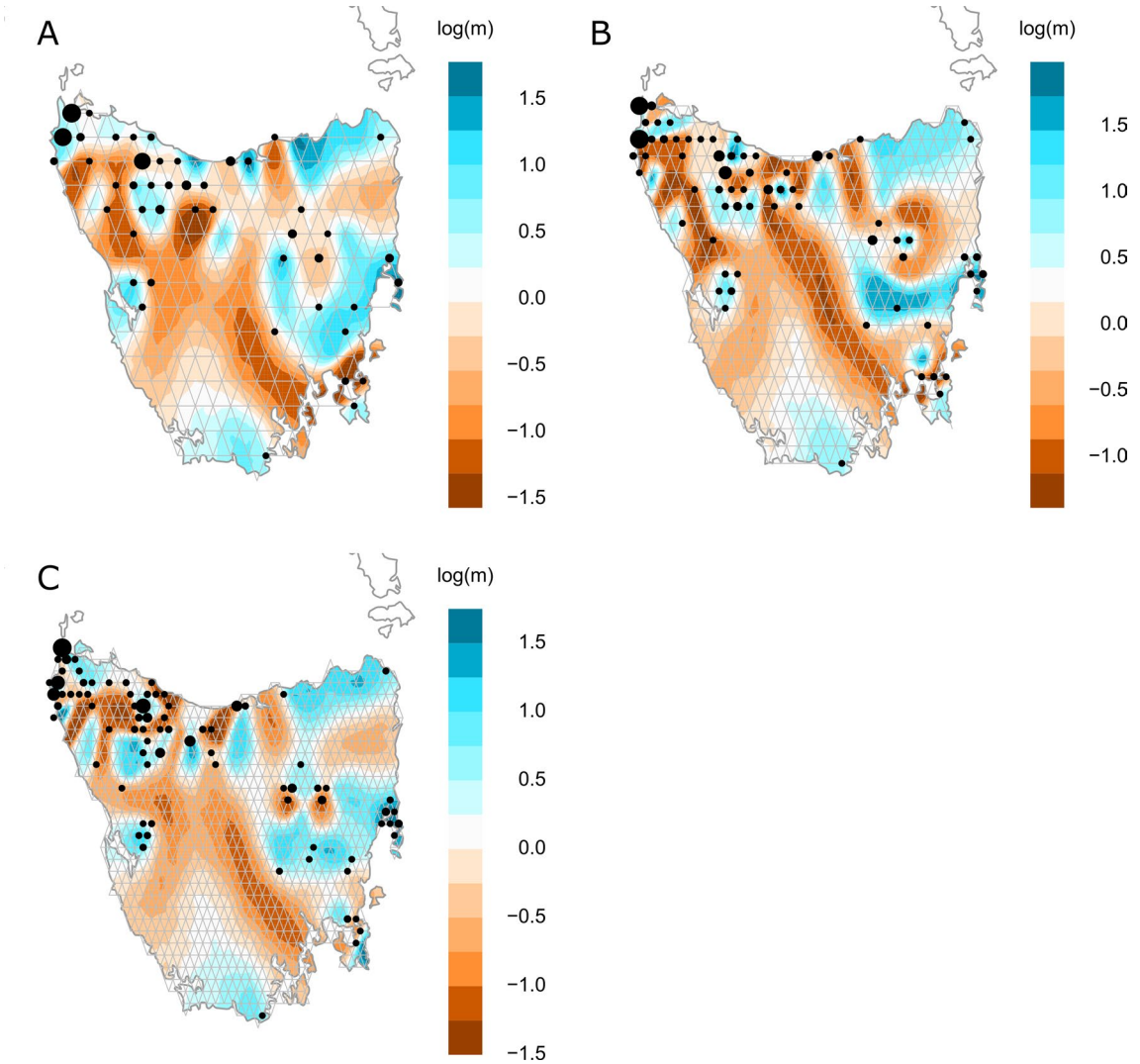

Extended Data Fig. 3 | EEMS plots of effective migration rates. Effective migration rate surfaces were determined for **a**) 250-, **b**) 500-, and **c**) 1000-deme lattices. Color indicates regions where effective migration is higher (blue) or lower (orange) than expected under a model of isolation by distance.

https://doi.org/10.1038/s41559-023-02265-9

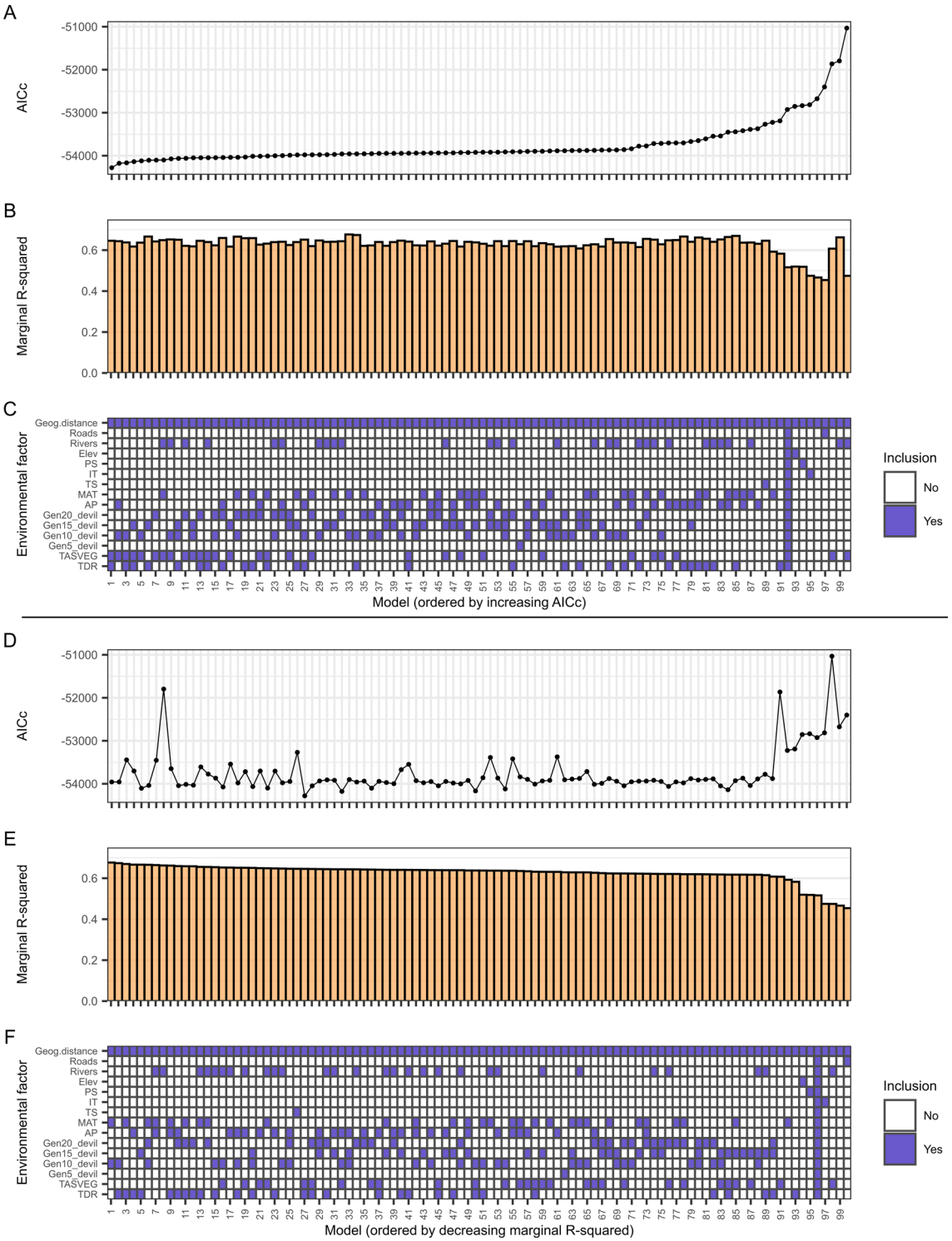

Extended Data Fig. 4 | All 100 linear mixed effects models with maximum likelihood population effects evaluating the contribution of abiotic and biotic variables to isolation-by-resistance. a–**c**) Models ordered left-to-right by increasing (worsening) AICc. **d**–**f**) Models ordered left-to-right by decreasing (worsening) marginal R-squared left to right. A, D) Average AICc of models based on 10,000 bootstrap replicates. B, E) Average marginal R-squared of models. Marginal R-squared is the proportion of variance in pairwise individual genetic distances explained by a resistance surface representing the composite of the indicated variables. C, F) Matrix indicating inclusion of environmental variables in each model. Isothermality (IT), TS (temperature seasonality), mean annual temperature (MAT), annual precipitation (AP), devil density lagged by 20, 15, 10, and 5 quoll generations (for example, Gen20_devil), landcover classes (TASVEG) and temperature diurnal range (TDR) are abbreviated in the matrix.

https://doi.org/10.1038/s41559-023-02265-9

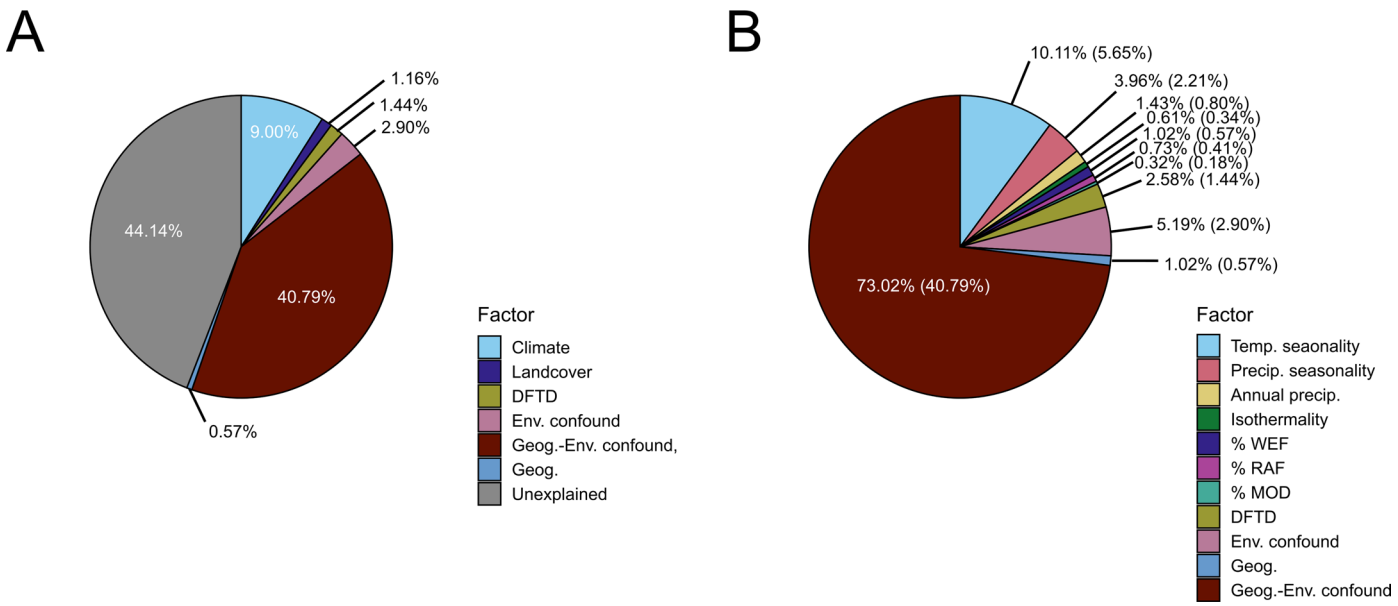

Extended Data Fig. 5 | Partitioning of model deviance in GDM. a) Percentages of *total model deviance* attributable to different factors, with individual environmental factors collapsed into climate, landcover, and generations diseased (DFTD). **b**) Percentages of *deviance explained* attributable to individual environmental factors and geography. Percentages in parentheses indicate contributions to total model deviance. Some explained deviance cannot be attributed uniquely to geography versus the environment (Geog-Env confound) or can be attributed uniquely to the environment but not individual environmental factors (Env. Confound).

https://doi.org/10.1038/s41559-023-02265-9

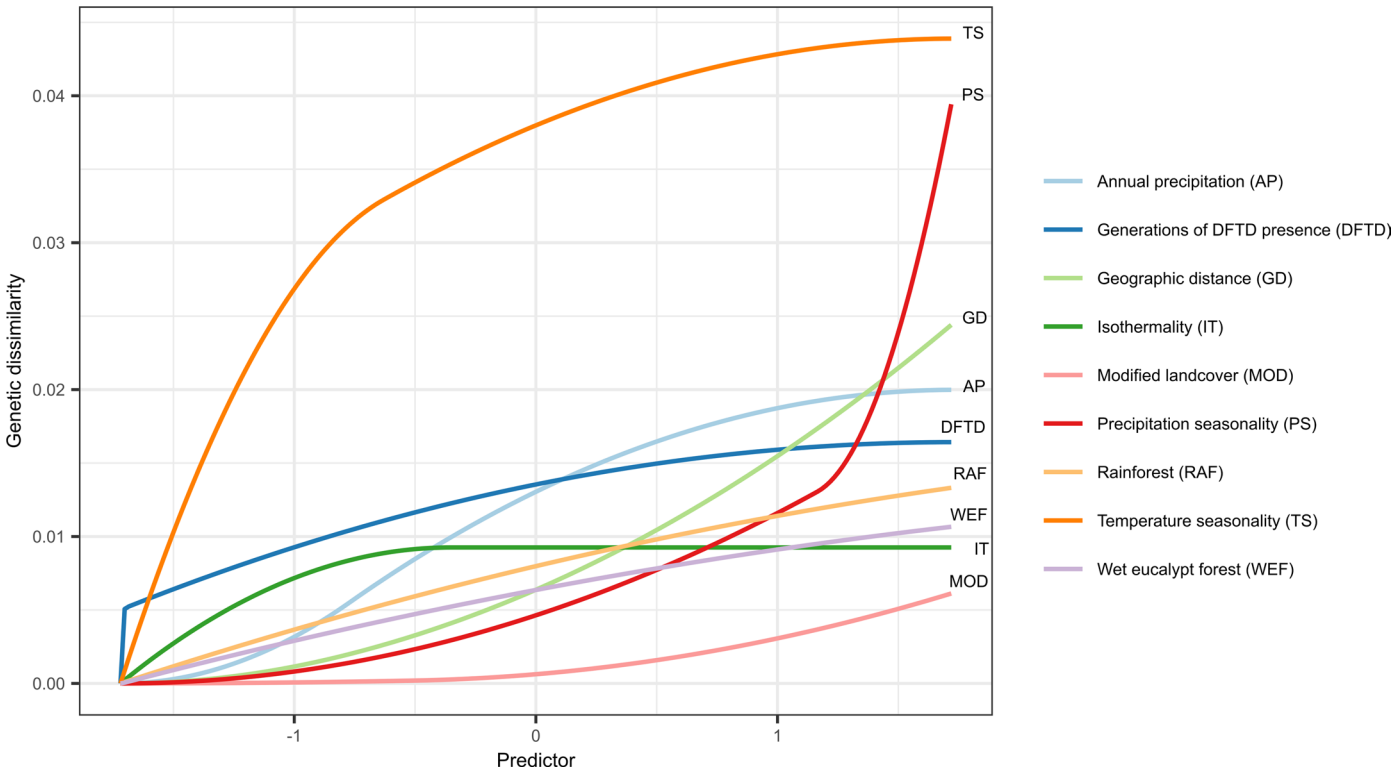

Extended Data Fig. 6 | GDM splines relating pairwise genetic distance to pairwise environmental differences. Environmental factors were centered and scaled by standard deviation to enable plotting on the same axes.

https://doi.org/10.1038/s41559-023-02265-9

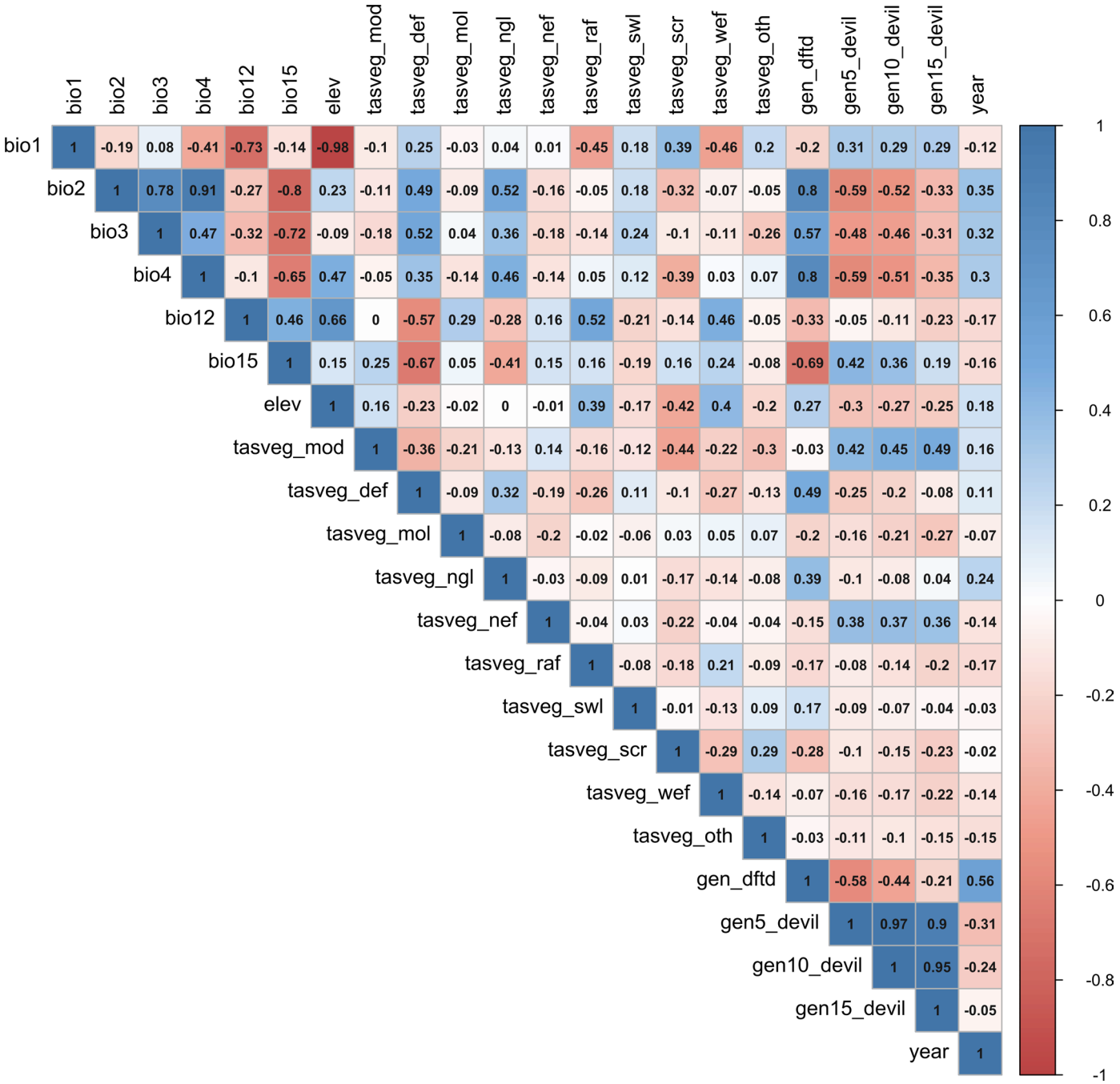

Extended Data Fig. 7 | Pearson's correlation coefficients for pairs of environmental factors. Numbers indicate the value of Pearson's correlation coefficient for a pair of environmental factors. Blue colours indicate positive values and red colours indicate negative values of Pearson's correlation coefficient.

https://doi.org/10.1038/s41559-023-02265-9

Extended Data Table 1 | Iterative filtering of spotted-tailed quoll genomic data

Step	Filtering mechanism	Value	Individual quolls remaining	SNPs remaining	Rationale	Software
1	Sequence read MAPQ	10	548	N/A	Remove RAD loci representing collapsed paralogs	Samtools
2	Max. heterozygosity	0.7	548	1,159,291	Remove SNPs derived from RAD loci representing collapsed paralogs	Stacks v2.52
3	Minimum global genotyping rate	0.1	548	1,159,291	Remove RAD loci with poor global representation	Stacks v2.52
4	Minimum spatiotemporal groups represented	100%	548	1,159,291	Retain RAD loci represented in all three geographic regions and all three time slices	Stacks v2.52
5	Retain individuals with precise geographic coordinates and sampling dates	N/A	440	1,159,291	Landscape genetics analysis requirement	VCFtools
6	Min. read depth to call a genotype	5	440	1,159,291	Reduce genotype miscalls	VCFtools
7	Min. minor allele count	3	440	537,919	Remove artefactual SNPs	VCFtools
8	Min. mean read depth	15	440	100,290	Reduce genotype miscalls	VCFtools
9	Individual missingness†	0.999	433	100,290	Reduce missing data	VCFtools
10	Spatiotemporal SNP missingness‡	0.7	433	97,636	Reduce missing data; reduce spatiotemporal bias in missing data	VCFtools
11	Individual missingness	0.95	422	97,636	Reduce missing data	VCFtools
12	Spatiotemporal SNP missingness	0.58	422	82,082	Reduce missing data; reduce spatiotemporal bias in missing data	VCFtools
13	Individual missingness	0.8	403	82,082	Reduce missing data	VCFtools
14	Spatiotemporal SNP missingness	0.46	403	72,724	Reduce missing data; reduce spatiotemporal bias in missing data	VCFtools
15	Individual missingness	0.65	383	72,724	Reduce missing data	VCFtools
16	Spatiotemporal SNP missingness	0.34	383	58,996	Reduce missing data; reduce spatiotemporal bias in missing data	VCFtools
17	Individual missingness	0.5	358	58,996	Reduce missing data	VCFtools
18	Minor allele frequency	0.03	358	5,191	Reduce confounding of genetic-environment association tests	VCFtools
19	One SNP per 5000bp	N/A	358	3,461	Reduce linkage among SNPs	VCFtools
20	Remove X-chromosome SNPs	N/A	358	3431	Ploidy assumptions	VCFtools
21	Remove individuals with putatively erroneous metadata	N/A	345	3431	Avoid confounding analyses with erroneous metadata	VCFtools

† Individual missingness refers to the removal of individuals that have a missing genotype rate higher than the specified value. ‡ Spatiotemporal SNP missingness refers to the removal of a SNP when its missing data rate exceeds the specified value in at least one of nine spatiotemporal groups of samples (see Materials and Methods).

https://doi.org/10.1038/s41559-023-02265-9

Extended Data Table 2 | Environmental factors considered for analyses

Environmental factor	Abbreviation†	IBE:pRDA‡	IBE:GDM‡	IBR‡	GEA:pRDA‡	GEA:LFMM‡
Mean annual temperature (Bio1)	MAT			x	x	x
Temperature diurnal range (Bio2)	TDR			x	x	x
Isothermality (Bio3)	IT	x	x	x		
Temperature seasonality (Bio4)	TS	x	x	x	x	x
Annual precipitation (Bio12)	AP	x	x	x	x	x
Precipitation seasonality (Bio15)	PS		x	x	x	x
Elevation	ELEV	x	x	x		
Rivers				x		
Roads				x		
TASVEG (categorical landcover)	TASVEG			x		
TASVEG dry eucalypt forest (proportion)	TASVEG_Def	x	x			
TASVEG moorland (proportion)	TASVEG_Mol	x	x			
TASVEG native grassland (proportion)	TASVEG_Ngl	x	x			
TASVEG non-eucalypt forest (proportion)	TASVEG_Nef	x	x			
TASVEG rainforest (proportion)	TASVEG_Raf	x	x			
TASVEG, saltmarsh wetland (proportion)	TASVEG_Swl	x	x			
TASVEG scrub (proportion)	TASVEG_Scr	x	x			
TASVEG wet eucalypt forest (proportion)	TASVEG_Wef	x	x			
TASVEG human-modified landcover (proportion)	TASVEG_Mod		x			
TASVEG other landcover (proportion)	TASVEG_Oth		x			
TASVEG highland treeless vegetation (proportion)	TASVEG_Htv					
Devil density, 5 generations lagged	Gen5_Devil			x		
Devil density, 10 generations lagged	Gen10_Devil	x		x	x	x
Devil density, 15 generations lagged	Gen15_Devil		x	x		
Devil density, 20 generations lagged	Gen20_devil			x		
Generations diseased	DFTD	x	x		x	x

† Abbreviations are shared with other tables and figures. ‡ Used in final analysis after removing factors based on VIFs or pairwise Pearson correlation coefficients.

https://doi.org/10.1038/s41559-023-02265-9

Extended Data Table 3 | Numbers of SNPs detected as significantly associated with environmental factors using pRDA and LFMM

Environmental factor	pRDA	LFMM	Total
Mean annual temperature	9	5	14
Mean temperature diurnal range	8	10	18
Temperature seasonality	18	13	31
Annual precipitation	14	28	41
Precipitation seasonality	18	35	50
TASVEG_Def	0	1	1
TASVEG_Mol	1	3	4
TASVEG_Ngl	2	4	6
TASVEG_Nef	1	0	1
TASVEG_Raf	0	5	5
TASVEG_Swl	2	10	12
TASVEG_Scr	2	4	6
TASVEG_Wef	4	0	4
Generations diseased	5	5	10
Devil density lagged 10 generations	8	6	12
Total	92	116	197

Bottom peripheral cells indicate the total number of significant SNPs detected using either pRDA or LFMM. Right-hand peripheral cells indicate the total number of significant SNPs detected by pRDA and LFMM for a given environmental factor. The bottom right cell indicates the total number of significant SNPs detected by pRDA and LFMM across all environmental factors. Totals are not universally the sum of adjacent cells because significant SNPs overlapped across methods and environmental factors.

nature portfolio

Corresponding author(s): Andrew Storfer

Last updated by author(s): Nov 2, 2023

Reporting Summary

Nature Portfolio wishes to improve the reproducibility of the work that we publish. This form provides structure for consistency and transparency in reporting. For further information on Nature Portfolio policies, see our Editorial Policies and the Editorial Policy Checklist.

Statistics

For all statistical analyses, confirm that the following items are present in the figure legend, table legend, main text, or Methods section.

n/a	Confirmed	
☐	☒	The exact sample size (*n*) for each experimental group/condition, given as a discrete number and unit of measurement
☒	☐	A statement on whether measurements were taken from distinct samples or whether the same sample was measured repeatedly
☐	☒	The statistical test(s) used AND whether they are one- or two-sided *Only common tests should be described solely by name; describe more complex techniques in the Methods section.*
☐	☒	A description of all covariates tested
☐	☒	A description of any assumptions or corrections, such as tests of normality and adjustment for multiple comparisons
☐	☒	A full description of the statistical parameters including central tendency (e.g. means) or other basic estimates (e.g. regression coefficient) AND variation (e.g. standard deviation) or associated estimates of uncertainty (e.g. confidence intervals)
☐	☒	For null hypothesis testing, the test statistic (e.g. *F*, *t*, *r*) with confidence intervals, effect sizes, degrees of freedom and *P* value noted *Give P values as exact values whenever suitable.*
☒	☐	For Bayesian analysis, information on the choice of priors and Markov chain Monte Carlo settings
☒	☐	For hierarchical and complex designs, identification of the appropriate level for tests and full reporting of outcomes
☐	☒	Estimates of effect sizes (e.g. Cohen's *d*, Pearson's *r*), indicating how they were calculated

Our web collection on statistics for biologists contains articles on many of the points above.

Software and code

Policy information about availability of computer code

Data collection	No software was used in data collection.
Data analysis	Software used in data analysis are described in detail, with associated references, in the Methods section. No custom algorithms or software were used in the research. Sequence data were processed using a combination of Cutadapt 4.2, Stacks v2.52,and BWA 0.7.17 to generate SNP genotypes. SNP genotypes were filtered for quality using VCFTools. Environmental data were processed in R 4.1, and QGIS 3.16.14 with GRASS 7.8.5. The analyses DAPC, ResistanceGA, sPCA, pRDA, GDM, and LFMM were conducted in R 4.1 using packages described in the Methods. Figures were created using ggplot2 in R 4.1 and Inkscape 1.1. The analysis FastStructure used version 1.0, and the analysis EEMS used version 1.0. Code underlying analyses has been deposited in a GitHub repository (https://github.com/marcabeer/stquoll_landscape_genomics).

For manuscripts utilizing custom algorithms or software that are central to the research but not yet described in published literature, software must be made available to editors and reviewers. We strongly encourage code deposition in a community repository (e.g. GitHub). See the Nature Portfolio guidelines for submitting code & software for further information.

Data

Policy information about availability of data

All manuscripts must include a data availability statement. This statement should provide the following information, where applicable:

- Accession codes, unique identifiers, or web links for publicly available datasets
- A description of any restrictions on data availability
- For clinical datasets or third party data, please ensure that the statement adheres to our policy

Sequence data and sample metadata necessary for reproducing the study have been deposited at NCBI under BioProject PRJNA922561 (https://dataview.ncbi.nlm.nih.gov/object/PRJNA922561?reviewer=k665j7vuqj8hum6io4jklkki48) and BioSamples SAMN32664143—32664814. Note that this link is a temporary reviewer link and full public access will be granted following publication. Any other relevant data can be found within the article and its supplementary information.

Research involving human participants, their data, or biological material

Policy information about studies with human participants or human data. See also policy information about sex, gender (identity/presentation), and sexual orientation and race, ethnicity and racism.

Reporting on sex and gender	*Use the terms sex (biological attribute) and gender (shaped by social and cultural circumstances) carefully in order to avoid confusing both terms. Indicate if findings apply to only one sex or gender; describe whether sex and gender were considered in study design; whether sex and/or gender was determined based on self-reporting or assigned and methods used.* *Provide in the source data disaggregated sex and gender data, where this information has been collected, and if consent has been obtained for sharing of individual-level data; provide overall numbers in this Reporting Summary. Please state if this information has not been collected.* *Report sex- and gender-based analyses where performed, justify reasons for lack of sex- and gender-based analysis.*
Reporting on race, ethnicity, or other socially relevant groupings	*Please specify the socially constructed or socially relevant categorization variable(s) used in your manuscript and explain why they were used. Please note that such variables should not be used as proxies for other socially constructed/relevant variables (for example, race or ethnicity should not be used as a proxy for socioeconomic status).* *Provide clear definitions of the relevant terms used, how they were provided (by the participants/respondents, the researchers, or third parties), and the method(s) used to classify people into the different categories (e.g. self-report, census or administrative data, social media data, etc.)* *Please provide details about how you controlled for confounding variables in your analyses.*
Population characteristics	*Describe the covariate-relevant population characteristics of the human research participants (e.g. age, genotypic information, past and current diagnosis and treatment categories). If you filled out the behavioural & social sciences study design questions and have nothing to add here, write "See above."*
Recruitment	*Describe how participants were recruited. Outline any potential self-selection bias or other biases that may be present and how these are likely to impact results.*
Ethics oversight	*Identify the organization(s) that approved the study protocol.*

Note that full information on the approval of the study protocol must also be provided in the manuscript.

Field-specific reporting

Please select the one below that is the best fit for your research. If you are not sure, read the appropriate sections before making your selection.

☐ Life sciences ☐ Behavioural & social sciences ☒ Ecological, evolutionary & environmental sciences

For a reference copy of the document with all sections, see nature.com/documents/nr-reporting-summary-flat.pdf

Ecological, evolutionary & environmental sciences study design

All studies must disclose on these points even when the disclosure is negative.

Study description	This study concerns the population genetics of the spotted-tailed quoll (Dasyurus maculatus) across Tasmania, Australia. Our data are quantitative and analyses typically used regression modeling methods to understand how environmental factors impact genetic variation in the study species.
Research sample	The initial dataset consisted of 548 unique samples of the spotted tailed quoll (Dasyurus maculatus), which were collected 2004—2019 across Tasmania, Australia. Samples were geographically and temporally widespread to capture the distribution of abiotic and biotic environmental conditions encountered by the study species. The final dataset consisted of 345 samples that were similarly geographically widespread as the initial dataset and spanned 2004—2017.
Sampling strategy	Sample size was not predetermined, as samples were collected opportunistically several years prior to conception of the study. Samples best conform to a random spatial sampling procedure, as samples are geographically widespread and represent a range of

	environmental conditions. The final dataset containing 345 geographically widespread samples exceeds recommendations based on landscape genomics simulations, which show that ≥200 samples are typically sufficient to achieve high statistical power (Selmoni et al., 2020; https://doi.org/10.1111/1755-0998.13095).
Data collection	Tissue samples were collected by the University of Tasmania and the Department of Natural Resources and Environment Tasmania. Individuals were caught in baited pipe traps. All individuals caught were implanted with a subcutaneous microchip to allow individual identification and had a 3mm biopsy (Kai Medical TM) taken from the lower edge of their right ear. Staff involved in sample collection were blind to the study hypothesis because this study was conceived several years after sample collection.
Timing and spatial scale	Sample collection dates spanned 2004—2019, with the final dataset spanning 2004—2017. All years except for 2015, which was not sampled, were represented by ≥2 samples; the mean number of samples for a given year was 24.6 samples (S.D. = 17.8 samples; max = 60 samples in 2012). Samples spanned the island of Tasmania, Australia, as depicted in Figure 2A. The mean distance between samples was 121km (S.D. = 91km; max = 373km).
Data exclusions	Genotype data were filtered to remove single nucleotide polymorphisms (SNPs) with high missing data across samples, as well as to remove samples with high missing data across SNPs. Samples lacking specific geographic coordinates or collection dates were also excluded following genotyping. This procedure, including missing data thresholds, is described in Extended Data Table 1. Missing data thresholds were predetermined such that they resulted in a final, nominal missing data rate of <50% on a per-SNP and per-sample basis, which is typical in the field of landscape genomics.
Reproducibility	Analyses characterized by stochasticity were repeated multiple times to ensure reliability, as described in the Methods.
Randomization	Randomization was not relevant to the study, as we applied analyses uniformly to the entire sample set.
Blinding	Blinding was not relevant to the study, as we applied analyses uniformly to the entire sample set.

Did the study involve field work? ☒ Yes ☐ No

Field work, collection and transport

Field conditions	Field conditions were not recorded during field work. General location and when possible, specific geographic coordinates were recorded.
Location	Sampling was conducted across the island of Tasmania, Australia. There were numerous (>300) unique geographic coordinates for samples, which are provided in the repository to which our data have been deposited.
Access & import/export	Field collections occurred across the island of Tasmania, Australia, at numerous locations. We complied with University of Tasmania Animal Ethics Permits (A0008588, A0010296, A0011696, A0013326, A0015835, A0018223, A0016789), as described in the Methods.
Disturbance	Individuals were captured in baited pipe traps that did not cause physical harm. Tissue samples were collected as 3mm ear biopsies to cause minimal damage to the individual. Individuals were released following implantation of a subcutaneous microchip and tissue collection. Handling procedures took 5-10min.

Reporting for specific materials, systems and methods

We require information from authors about some types of materials, experimental systems and methods used in many studies. Here, indicate whether each material, system or method listed is relevant to your study. If you are not sure if a list item applies to your research, read the appropriate section before selecting a response.

Materials & experimental systems

n/a	Involved in the study
☒	☐ Antibodies
☒	☐ Eukaryotic cell lines
☒	☐ Palaeontology and archaeology
☐	☒ Animals and other organisms
☒	☐ Clinical data
☒	☐ Dual use research of concern
☒	☐ Plants

Methods

n/a	Involved in the study
☒	☐ ChIP-seq
☒	☐ Flow cytometry
☒	☐ MRI-based neuroimaging

Animals and other research organisms

Policy information about studies involving animals; ARRIVE guidelines recommended for reporting animal research, and Sex and Gender in Research

Laboratory animals	The study did not involve laboratory animals.
Wild animals	The study involved temporary capture of individual spotted-tailed quolls (Dasyurus maculatus) across Tasmania, Australia. Individuals were released following microchipping and tissue sample collection on-site.
Reporting on sex	Findings apply to both sexes, as they were analysed together throughout the study. The initial 548 individuals included 330 males, 160 females, and 182 individuals of unknown sex. The final dataset of 345 individuals included 213 males, 101 females, and 31 individuals of unknown sex. Population genetic analyses do not typically stratify samples by sex.
Field-collected samples	Individuals were not taken into the laboratory. Samples were collected in the form of preserved tissue biopsies.
Ethics oversight	Ethics oversight was provided by the University of Tasmania Animal Ethics and the Tasmania Department of Natural Resources and Environment Ethics Committees.

Note that full information on the approval of the study protocol must also be provided in the manuscript.